FINAL TECHNICAL REPORT

Paleoseismic Investigation of the Simi fault, Ventura County, California

by
Christopher S. Hitchcock[1], Scott C. Lindvall[2], Jerome A. Treiman[3], Kristin D. Weaver[2], John G. Helms[2], and William R. Lettis[1]

[1]William Lettis & Associates, Inc.
1777 Botelho Drive, Suite 262
Walnut Creek, California 94596
phone: (925) 256-6070; fax: (925) 256-6076
e-mail: hitch@lettis.com

[2]William Lettis & Associates, Inc.
25050 Avenue Kearny #108
Valencia, California 91355
phone: (661) 775-4990; fax: (661) 775-4993
e-mail: lindvall@lettis.com

[3]655 S. Hope Street, #700
Los Angeles, CA 90017
phone: (213) 239-0878 fax: (213) 239-0894
Dept. of Conservation, Div. Mines and Geology
e-mail: jtreiman@consrv.ca.gov

February 2001

TABLE OF CONTENTS

List of Figures

FINAL TECHNICAL REPORT

Paleoseismic Investigation of the Simi fault, Ventura County, California

Christopher S. Hitchcock[1], Scott C. Lindvall[2], Jerome A. Treiman[3], Kristin D. Weaver[2], John G. Helms[2], and William R. Lettis[1]

[1] William Lettis & Associates, Inc., 1777 Botelho Drive, Suite 262, Walnut Creek, California 94596; phone: (925) 256-6070; fax: (925) 256-6076; email: hitch@lettis.com

[2] William Lettis & Associates, Inc.; 25050 Avenue Kearny #108; Valencia, California 91355; phone: (661) 775-4990; fax: (661) 775-4993; email: lindvall@lettis.com

[3] Dept. of Conservation, Div. Mines and Geology; 655 S Hope Street, #700, Los Angeles, CA 90017; phone: (213) 239-0878 fax: (213) 239-0894; email: jtreiman@consrv.ca.gov

ABSTRACT

The Simi fault is a left-oblique reverse fault within the Simi-Santa Rosa fault zone, a series of north-dipping faults that trend southwest from the northeastern end of Simi Valley to the Oxnard plain in southern California. The Simi-Santa Rosa fault zone is one of a series of major reverse fault systems that accommodate folding and uplift of the west-trending Transverse Ranges. Large earthquakes on adjacent reverse faults beneath San Fernando Valley to the east produced the 1971 San Fernando and 1994 Northridge earthquakes, yet the seismogenic potential of the Simi-Santa Rosa fault zone is not well constrained. Results from our paleoseismic investigations at Arroyo Simi within Simi Valley provide information on the recency of fault activity, sense of slip, amount of displacement per event on the Simi fault, and allow us to estimate an average Holocene slip rate. We define the location of the main strand of the Simi fault based on detailed mapping, shallow boreholes, and documentation of stream and trench exposures along Arroyo Simi at the northwestern end of Simi Valley. Stream bank and trench excavations reveal a narrow zone of brittle and ductile faulting, up to 3-m-wide, consisting of sub-vertical Holocene-active strands. Drag folds within clay layers and faulted stratigraphic horizons document a component of reverse displacement across the fault. Reconstruction of a laterally offset late Holocene stream channel deposit, combined with well-developed slickensides and mullions on the main fault plane, indicate a component of left-lateral slip, suggesting that the fault has an overall left-lateral, reverse sense of slip. The most recent event probably occurred between about 1,350 ybp (age of an offset stream channel deposit) and 1,205 ybp (age of overlying unfaulted colluvium), or alternatively, based on a different stratigraphic interpretation, between 4520 to 4960 BP (the age of faulted clay deposits) and 2060 to 2360 BP (age of possibly unfaulted buried soils). Reconstruction of a faulted and warped clay marker bed and tilted buried soils suggest that the most recent event produced about 1 to 1.5 m of vertical separation, yielding 2 to 2.5 m of total oblique slip displacement. This amount of displacement per event is consistent with M_W 7 earthquakes. The available stratigraphic and age data at the site provide a broadly constrained estimate of Holocene slip rate of about 1 mm/yr.

TABLE OF CONTENTS (cont'd)

List of Tables

Appendix

FINAL TECHNICAL REPORT

Paleoseismic Investigation of the Simi fault, Ventura County, California

Christopher S. Hitchcock[1], Scott C. Lindvall[2], Jerome A. Treiman[3], Kristin D. Weaver[2], John G. Helms[2], and William R. Lettis[1]

[1] *William Lettis & Associates, Inc., 1777 Botelho Drive, Suite 262, Walnut Creek, California 94596; phone: (925) 256-6070; fax: (925) 256-6076; email: hitch@lettis.com*

[2] *William Lettis & Associates, Inc.; 25050 Avenue Kearny #108; Valencia, California 91355; phone: (661) 775-4990; fax: (661) 775-4993; email: lindvall@lettis.com*

[3] *Dept. of Conservation, Div. Mines and Geology; 655 S Hope Street, #700, Los Angeles, CA 90017;phone: (213) 239-0878 fax: (213) 239-0894; email: jtreiman@consrv.ca.gov*

ABSTRACT

The Simi fault is a left-oblique reverse fault within the Simi-Santa Rosa fault zone, a series of north-dipping faults that trend southwest from the northeastern end of Simi Valley to the Oxnard plain in southern California. The Simi-Santa Rosa fault zone is one of a series of major reverse fault systems that accommodate folding and uplift of the west-trending Transverse Ranges. Large earthquakes on adjacent reverse faults beneath San Fernando Valley to the east produced the 1971 San Fernando and 1994 Northridge earthquakes, yet the seismogenic potential of the Simi-Santa Rosa fault zone is not well constrained. Results from our paleoseismic investigations at Arroyo Simi within Simi Valley provide information on the recency of fault activity, sense of slip, amount of displacement per event on the Simi fault, and allow us to estimate an average Holocene slip rate. We define the location of the main strand of the Simi fault based on detailed mapping, shallow boreholes, and documentation of stream and trench exposures along Arroyo Simi at the northwestern end of Simi Valley. Stream bank and trench excavations reveal a narrow zone of brittle and ductile faulting, up to 3-m-wide, consisting of sub-vertical Holocene-active strands. Drag folds within clay layers and faulted stratigraphic horizons document a component of reverse displacement across the fault. Reconstruction of a laterally offset late Holocene stream channel deposit, combined with well-developed slickensides and mullions on the main fault plane, indicate a component of left-lateral slip, suggesting that the fault has an overall left-lateral, reverse sense of slip. The most recent event probably occurred between about 1,350 ybp (age of an offset stream channel deposit) and 1,205 ybp (age of overlying unfaulted colluvium), or alternatively, based on a different stratigraphic interpretation, between 4520 to 4960 BP (the age of faulted clay deposits) and 2060 to 2360 BP (age of possibly unfaulted buried soils). Reconstruction of a faulted and warped clay marker bed and tilted buried soils suggest that the most recent event produced about 1 to 1.5 m of vertical separation, yielding 2 to 2.5 m of total oblique slip displacement. This amount of displacement per event is consistent with M_W 7 earthquakes. The available stratigraphic and age data at the site provide a broadly constrained estimate of Holocene slip rate of about 1 mm/yr.

1.0 INTRODUCTION

The Simi fault is a south-vergent, left-oblique reverse fault of the Simi-Santa Rosa fault system, a series of north-dipping faults that trend southwest from the northeastern end of Simi Valley to the east edge of the Oxnard plain (Figure 1). Progressive westward rupture along thrust faults to the east (i.e., 1971 San Fernando and 1994 Northridge earthquakes) suggests that future large earthquakes may occur on thrust faults within the Simi Valley area. Although the Simi-Santa Rosa fault system is located within the hanging wall of the larger Oak Ridge reverse fault system (Huftile and Yeats, 1996), it is unclear how the Simi-Santa Rosa fault zone is related to the Oak Ridge fault system and to the Sierra Madre-Cucamonga thrust fault system to the east.

Regional probabilistic seismic hazard studies have incorporated hazard from the Simi-Santa Rosa fault system using broad assumptions based on minimal available paleoseismic data. Petersen et al. (1996) assigned a M6.8 earthquake on the Simi-Santa Rosa fault system based on an estimated 36-km fault length. A slip rate of 0.7 mm/yr ($\pm$ 0.3 mm/yr) obtained from the Springville fault (Gonzalez and Rockwell, 1991), has generally been used to characterize the entire Simi-Santa Rosa fault system (WGCEP, 1995; Petersen et al., 1996). However, this slip rate, obtained from vertical dip-slip separation across a fault splay at the western end of the fault system, may not be representative of the entire system.

In this paper, we provide results from our paleoseismic investigation of the Simi-Santa Rosa fault near Arroyo Simi, in Simi Valley, California (Figure 2). At this location, the fault is exposed within the stream banks of Arroyo Simi and the main fault trace is defined by fault gouge juxtaposing Sespe bedrock against warped and faulted Holocene clay layers. Results of our study document the location, style, and timing of Holocene activity on the Simi-Santa Rosa fault, place constraints on the amount of displacement during the most recent and penultimate events, and allow us to make an approximate estimate of slip rate. These data are important for estimating earthquake probabilities in the greater Los Angeles metropolitan area (e.g. WGCEP, 1995), assessing regional strain-rate budgets, and evaluating local seismic hazards for general community planning. In addition, these data provide important constraints on the tectonic setting of the Simi-Santa Rosa fault and the role of the fault in accommodating strain within the Transverse Ranges.

2.0 TECTONIC SETTING

Regional uplift in the Transverse Ranges, resulting from crustal contraction across the large bend in the San Andreas fault, is accommodated by uplift of west-trending mountain ranges above major reverse faults. These fault systems include the Oak Ridge and Sierra Madre-Cucamonga fault systems, that extend from the San Andreas fault near San Bernardino to the western Santa Barbara Channel, and the Transverse Ranges Southern Boundary fault system (Dolan et al., 2000), that extends along the northern margin of the Los Angeles Basin and offshore along the Malibu Coast (Figure 1). Recent regional studies (e.g. Sorlien et al., 2000; Dolan et al., 2000) focused on the Oak Ridge and Santa Monica faults that bound the Santa Monica and Santa Susana Mountains and intervening east-west trending valleys. The mountainous area between these major fault systems is defined as a fairly rigid block (Argus et al., 1999), although several laterally extensive faults traverse the region including the inferred Santa Monica Mountains Thrust (Davis and Namson, 1994), and the Simi-Santa Rosa fault zone.

The north-dipping Simi-Santa Rosa fault zone is located within the hanging wall of the larger south-dipping Oak Ridge fault system (Huftile and Yeats, 1996). North of the Simi-Santa Rosa fault, the Santa Susana Mountains are intensely deformed by a series of active faults and folds, including the westward extension of the Santa Susana fault. South of the Simi-Santa Rosa fault system, relatively minor faulting, folding, and regional uplift is occurring based on recent studies
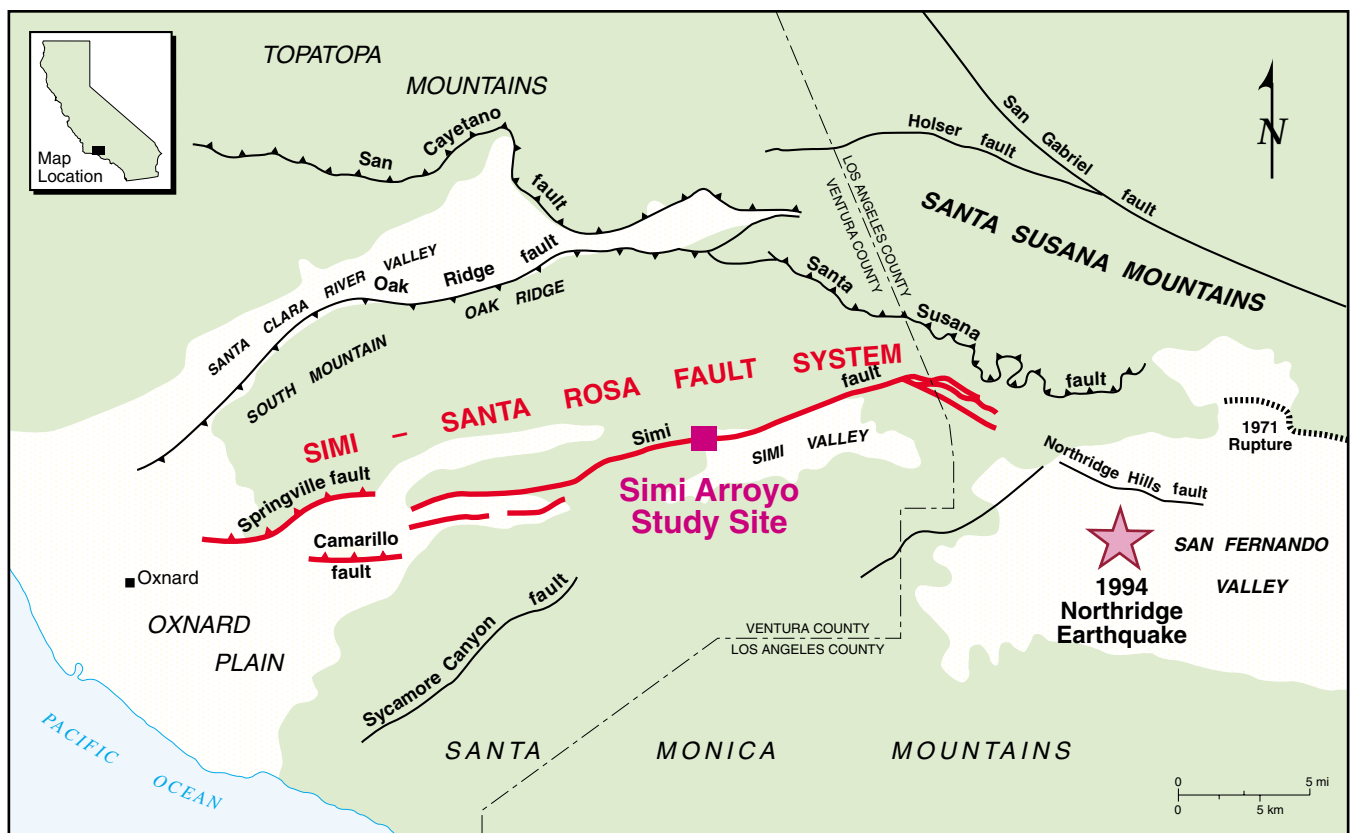
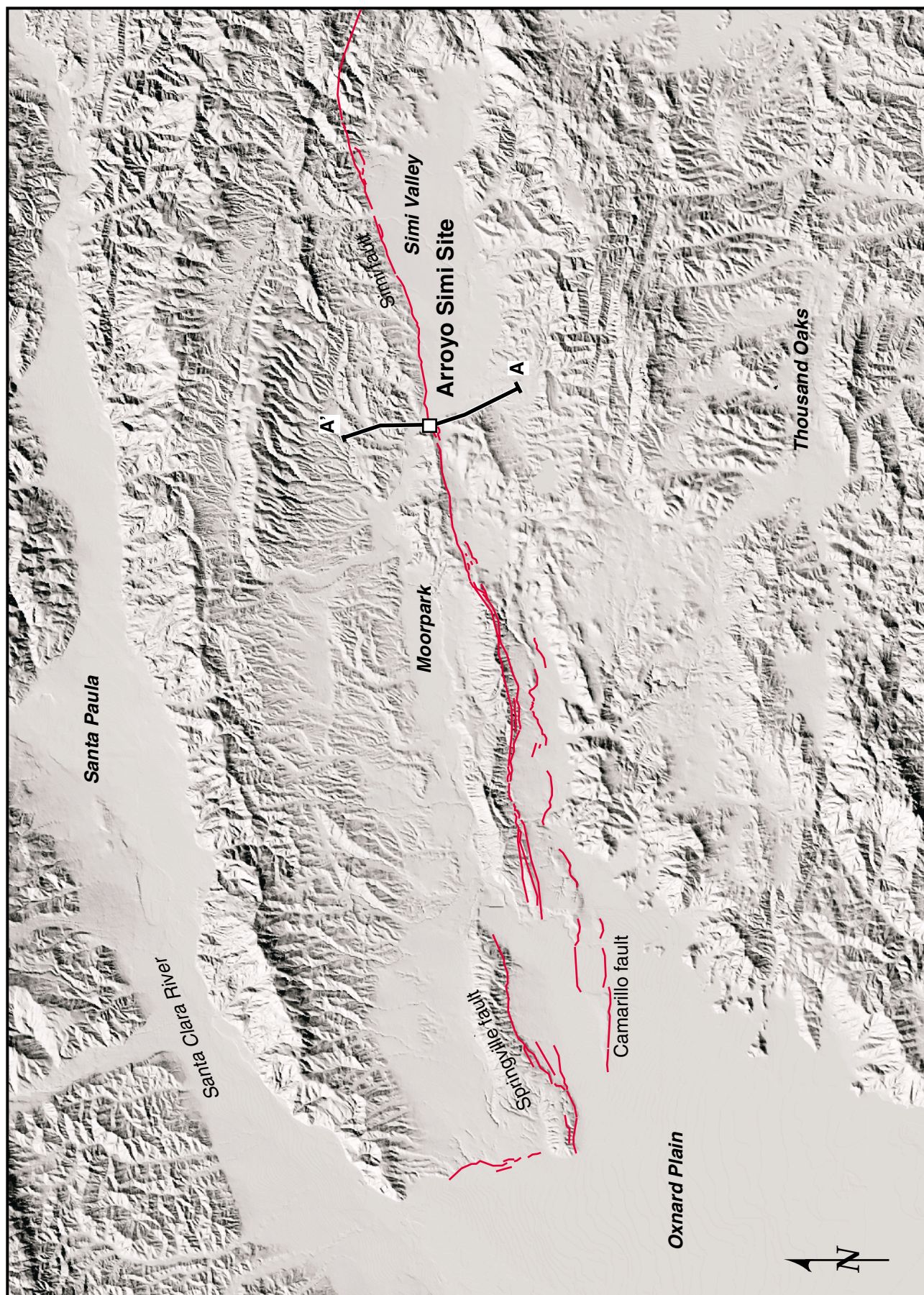Figure 1. Regional map showing location of the Arroyo Simi paleoseismic study site.

Figure 2. General shaded relief map showing Simi-Santa Rosa fault system and location of the Arroyo Simi paleoseismic site (fault traces from Treiman, 1999). Location of structural cross-section A-A' in Figure 3 is shown.

(Argus et al., 1999; Dolan et al., 2000). Davis et al. (1989) and Davis and Namson (1994) speculate that the Santa Monica Mountains are the surface expression of a fault-propagation fold above a south-vergent, north-dipping blind thrust fault later termed the Santa Monica blind thrust fault by Dolan et al. (1995). However, Dolan et al (2000) concluded that geologic and geophysical data suggest a very slow regional uplift rate for the Santa Monica Mountains north of the Santa Monica fault and that the Santa Monica blind thrust, if it exists, must be slipping at a rate much slower than that originally proposed by Davis and Namson (1994).

3.0 GEOLOGIC AND GEOMORPHIC SETTING

The 28-km-long, east-west trending Simi fault is located at the eastern end of the Simi-Santa Rosa fault zone. The north-dipping Simi fault bounds the northern margin of Simi Valley, forming a single, well-defined trace coincident with the range front. West of Tierra Rejada Valley, the Simi fault splits into at least two distinct strands (Figure 2). Near Camarillo, the Simi-Santa Rosa fault zone consists of several sub-parallel fault strands including the Springville and Camarillo faults.

Beneath Simi Valley, Tertiary and older sedimentary rocks are folded into the broad, west-plunging Simi syncline (Dibblee, 1992). The Simi syncline forms an east-west trending asymmetrical bedrock low filled with late Quaternary sediments derived from the surrounding mountains. The Simi syncline is truncated by the north-dipping Simi fault. Based on structural cross-sections constructed from oil-well data, the Simi fault is a high-angle fault dipping approximately 65 degrees in the upper 5 km (Hanson, 1981; Figure 3).

The relative distribution of strike-slip and reverse slip displacement on the Simi-Santa Rosa fault is poorly constrained. The 15.5 ± 0.8 m.y.a. base of the Conejo Volcanics, identified in oil well logs west of Simi Valley, is inferred to have a dip-slip separation of about 425 to 550 m, suggesting a long-term slip rate of about 0.03 mm/yr (Blake, 1991). However, substantial late Quaternary offset is suggested by the presence of more than 150 m of Pleistocene and younger alluvium that fills the east-west trending, down-dropped bedrock trough beneath western Simi Valley (Leighton and Associates, 1972; Yeats, 1983). This alluvium contains fine-grained marsh, shallow lake, and distal alluvial sand deposits that overlie coarser gravel deposits at depth (Leighton and Associates, 1972; Weber and others, 1973). The fine-grained deposits likely reflect sedimentation in floodplain and lacustrine environments formed when episodic displacements on the Simi fault caused blockage and ponding of Arroyo Simi (Yeats, 1983; Hitchcock and others, 1998).

Geomorphic evidence also suggests a significant component of sinistral slip on the Simi fault (Yeats, 1983; Blake, 1991). The Simi fault trace is well-expressed by scarps, faceted ridge spurs, deflected drainages, and linear topographic features across late Quaternary deposits (Blake, 1991; Treiman, 1999) that are typical of strike-slip faulting. In fact, the Simi fault is remarkably linear along much of its mapped length and coincident with a low-sinuosity mountain front along northern Simi Valley (Figure 2; Yeats, 1983; Blake, 1991). In addition, detailed geologic mapping (Hitchcock et al., 1999; Hitchcock et al., in prep.) documents possibly offset older alluvial fans that appear to lack sufficient drainage area near their inferred apices, consistent with significant lateral displacement. We conclude that the Simi fault is an oblique, left-lateral reverse fault.

The timing and recency of movement along the Simi fault also is poorly constrained. Prior to this study, the current state of activity on the Simi fault was unknown. Displacement of late Quaternary deposits across the Springville fault at the western end of the Simi-Santa Rosa fault zone previously was documented by Gonzalez and Rockwell (1991), and reported across the Simi fault in Simi and Tierra Rejada Valleys (Hanson, 1981; Swift, 1991; Blake, 1991). In the vicinity of Tapo Canyon in northeastern Simi Valley, the Simi fault juxtaposes Eocene Llajas Formation rocks against alluvial deposits of probable late Pleistocene age (Hanson, 1981). At Erringer Road approximately 4 km
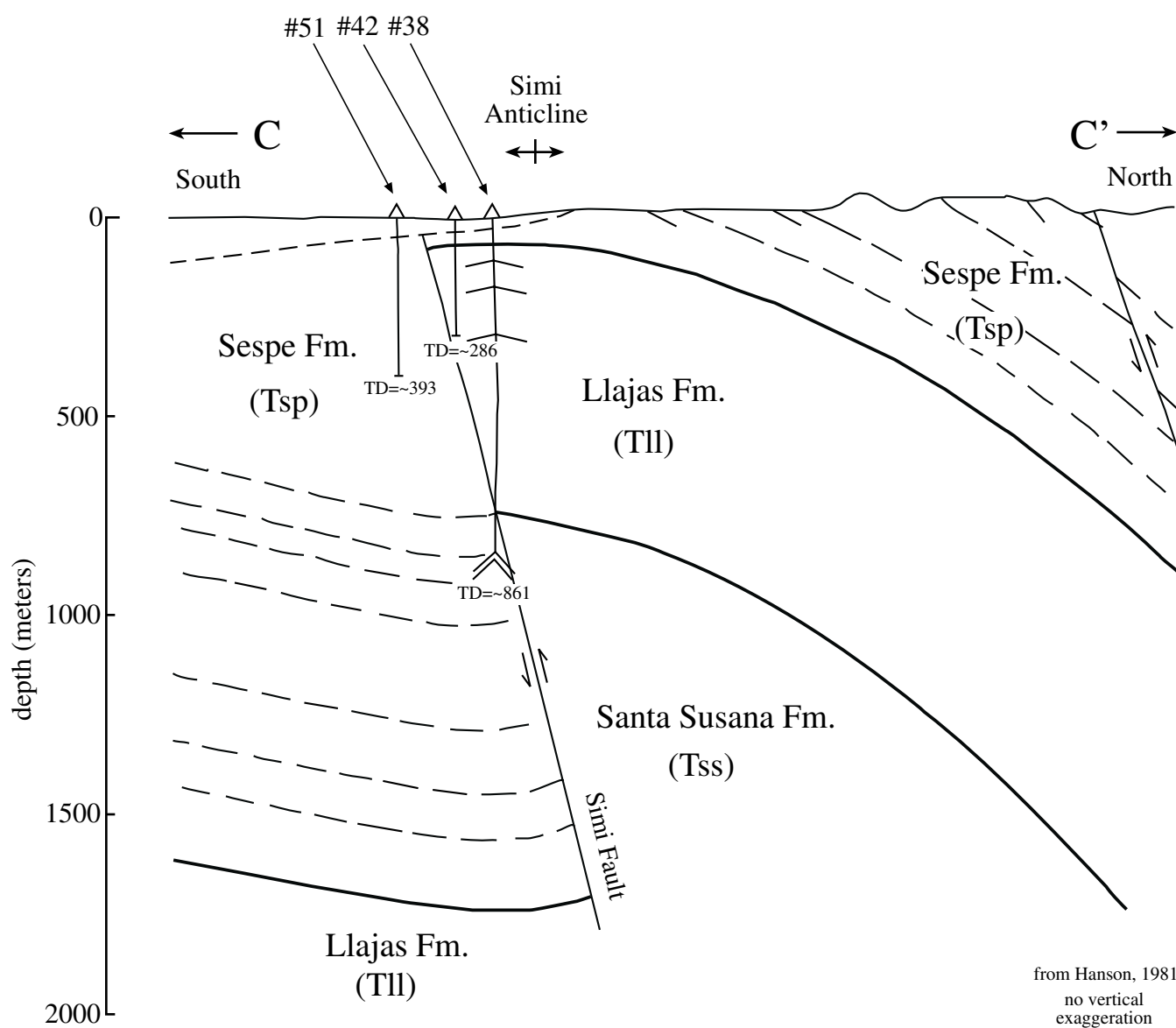
Figure 3. A portion of a cross section by Hanson (1981) constructed across the Arroyo Simi site illustrating the relationship of the Simi fault with the bedrock underlying the site.

west of the Arroyo Simi site, the fault juxtaposes late Eocene and Oligocene Sespe Formation bedrock against late Quaternary alluvium (Swift, 1991). Nearby deep exploratory excavations exposed shears within colluvial deposits suggestive of Holocene activity (Swift, 1991; Blake, 1991). Recently, based in part on preliminary results of our initial study at Arroyo Simi (Hitchcock et al., 1998) and upon compilation of previous consultant studies and detailed mapping of fault-related features (Treiman, 1999), the Simi-Santa Rosa fault zone has been zoned as active by the State of California (Treiman, 1999).

4.0 SITE DESCRIPTION

The Arroyo Simi paleoseismic site is located at the northwestern end of Simi Valley where Arroyo Simi exits Simi Valley (Figure 2). At this location, Arroyo Simi is confined to a narrow natural stream channel incised across the hanging wall of the Simi fault. Historic stream incision produced a 5- to 8-m-high exposure along the western stream bank. Holocene clay and silty clay deposits are exposed in fault contact with sandstone of the Sespe Formation at the base of the exposure. The fault extends upward into overlying Holocene laminated clay, silty clay, and gravelly sand deposits. Downstream of the fault exposure, within the hanging-wall of the fault, Arroyo Simi is incised into the folded and faulted Sespe bedrock and overlying silt and clay deposits that contain Pleistocene or younger fresh-water fossils (pers. comm., L. Groves, Los Angeles County Museum, 1997). These deposits are folded, consistent with late Quaternary uplift and folding of the hanging wall of the Simi fault.

Based on interpretation of 1938 black-and-white stereo-pair photographs and our field mapping, the Simi fault extends southwestward from the base of the linear range front bounding the northern margin of Simi Valley beneath Holocene fluvial fill terraces at the western end of Simi Valley (Figure 4). The younger Holocene terrace (unit Qyat2; Figure 4), located directly east of Arroyo Simi and the fault exposure appears to be unfaulted and is inset into older terrace remnants (unit Qyat1; Figure 4) that are present on both sides of the arroyo. Several south-facing, east-trending scarps are mapped within the older terrace (Qyat1) based on air-photo interpretation and pre-development contour maps. These scarps are on trend with the fault exposed in the Arroyo Simi stream bank, although the presence of a small knoll on historic photographs (since removed by grading) southwest of the exposure suggests that additional fault strands may be present to the south of the documented fault. Subtle east-west trending tonal and topographic lineaments within the Qyat1 surface coincide with the knoll and likely represent fault strands that bound the knoll.

Recent trenching investigations for proposed development at the old Simi Drive-In, located southwest of the Arroyo Simi paleoseismic site, exposed low-angle (<20°) north-dipping faults that offset bedrock and the overlying soil (Figure 5a). Based on the well-defined nature of the vertical fault trace exposed in the Arroyo Simi exposures, the near-vertical dip of the fault on structural cross-sections (Hanson, 1981; Figure 3), and likely secondary role of the low-angle features in strain partitioning (e.g. Lettis and Hanson, 1991), we conclude that the vertical strand documented in this study is the main fault strand. Thus we believe that most of the slip likely has occurred on the vertical strand. However, we can not preclude additional displacement on the low-angle strands south of the Arroyo Simi exposures.

5.0 METHODS

We mapped the tectonic geomorphology of the Simi fault in the vicinity of the Arroyo Simi site by interpretation of historical aerial photography and detailed geologic and geomorphic mapping. Our mapping incorporates geologic mapping by Hitchcock et al. (1999; in prep.) and mapping of fault-related features along the Simi fault for zoning of the fault as active by the State of California
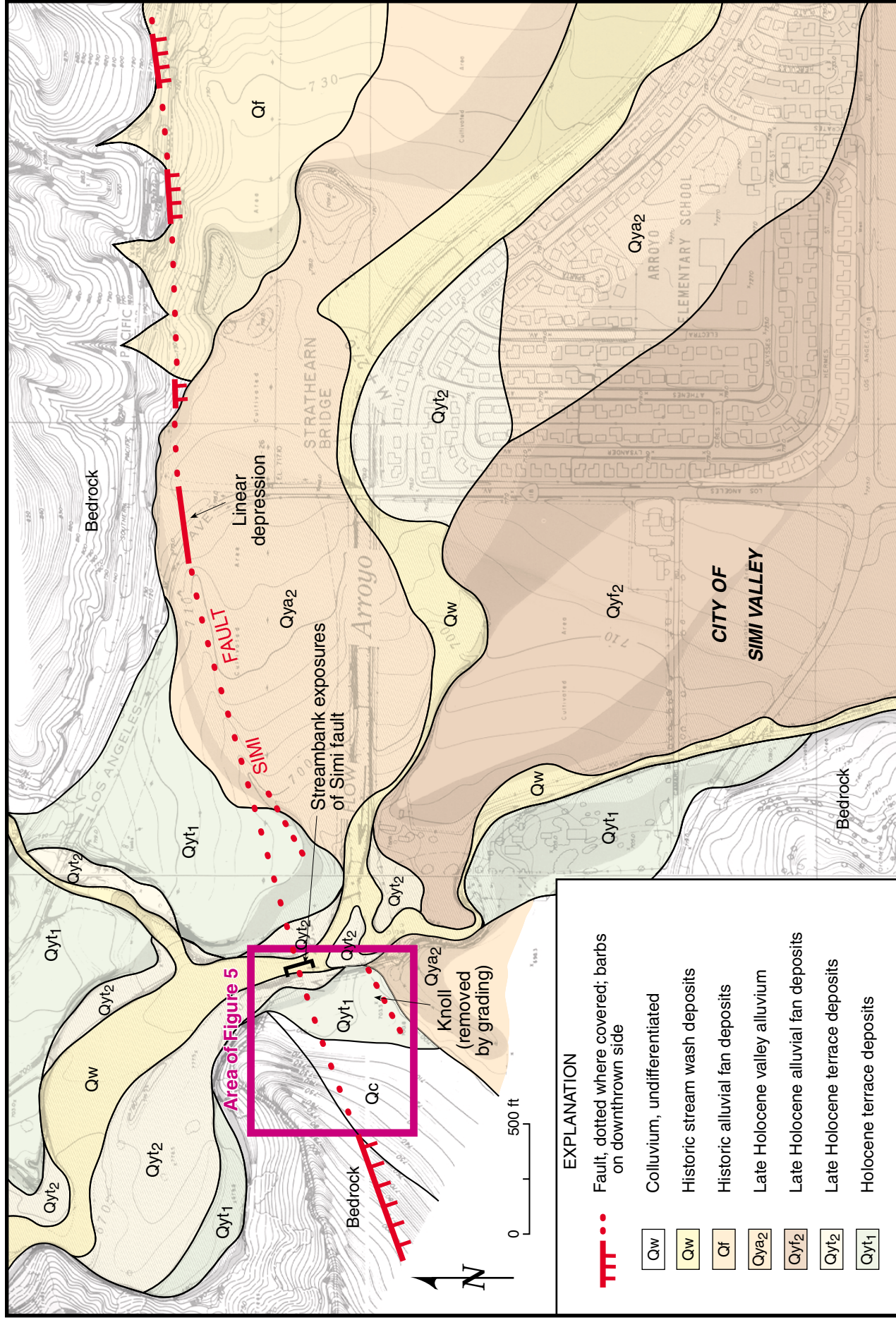
Figure 4. Map of surficial deposits and the Simi fault in the northwestern Simi Valley showing the Arroyo Simi study area. Topographic base map from the Ventura County Flood Control District, date of topography is 1967. Mapping is based on Hitchcock et al. (1999) and field mapping performed for this study.

EXPLANATION

Fault, dotted where covered; barbs on downthrown side

Qw — Colluvium, undifferentiated

Qw — Historic stream wash deposits

Qf — Historic alluvial fan deposits

Qya2 — Late Holocene valley alluvium

Qyf2 — Late Holocene alluvial fan deposits

Qyt2 — Late Holocene terrace deposits

Qyt1 — Holocene terrace deposits

Figure 5a. Site topographic map showing fault traces mapped at the Arroyo Simi paleoseismic site.

(Treiman, 1999). The mapping confirms that the fault within the Arroyo Simi stream exposures is a major fault strand of the Simi fault, coincident with the fault-bounded range front along the northern margin of Simi Valley and with linear geomorphic features within late Quaternary deposits (Figure 4).

We cleaned and documented two stream-cut exposures of the Simi fault, one in 1997 and the other in 2000 after flooding removed a portion of the pre-existing Arroyo Simi stream bank. The exposures were cleaned, gridded, and logged at scales of 1 in = 0.25m to 0.5m. We also conducted limited drilling to constrain the amount of vertical separation of late Pleistocene fluvial deposits across the Simi fault and improve our correlations of stratigraphic units. Ten 24-inch-diameter bucket auger holes were drilled, four within the hanging wall, downstream of the fault, and six within the foot wall, upstream of the fault (Figure 5b).

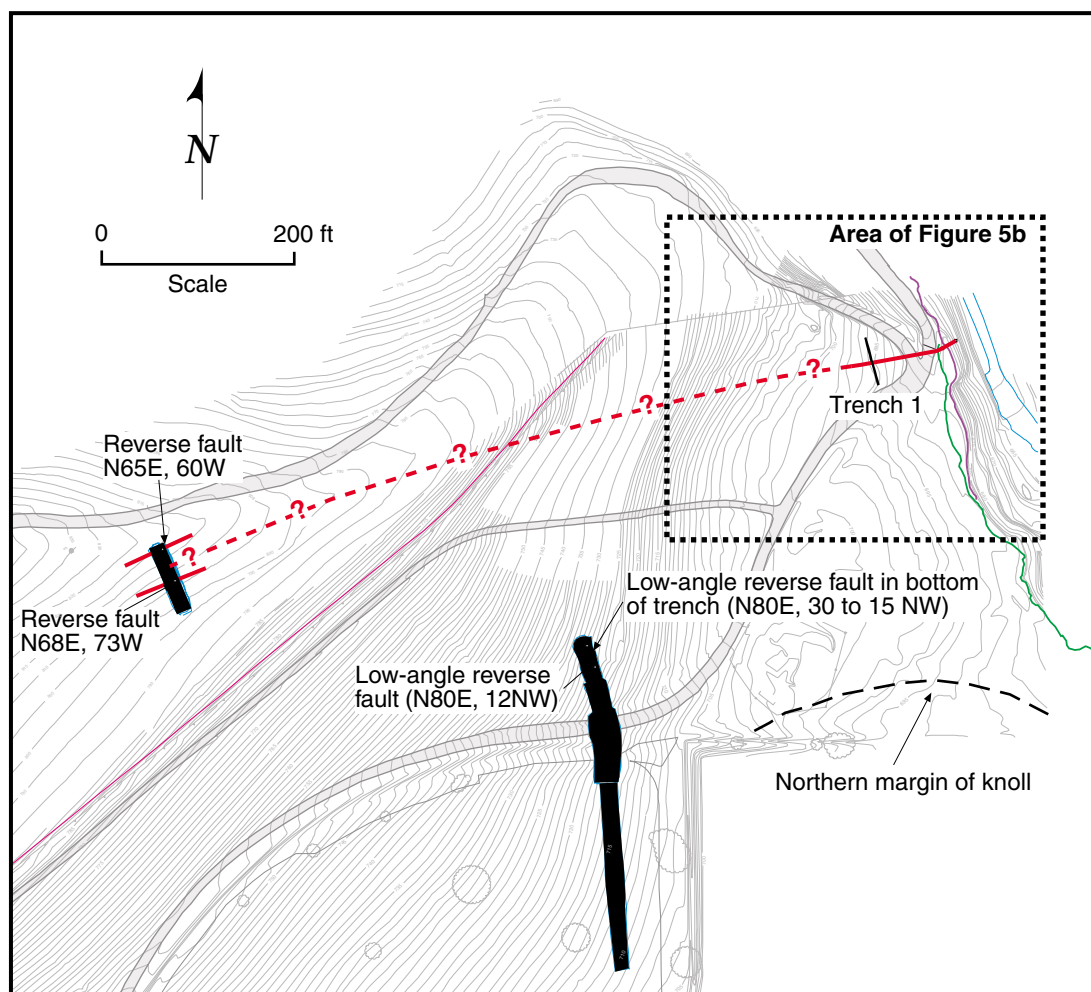Samples of detrital charcoal were submitted for radiocarbon analysis by accelerator mass spectrometry at Beta Analytic Inc., Miami, Florida (Table 1). The radiometric dates were dendrochronologically corrected to calibrated years according to the procedure of Stuiver and Reimer (1998). In addition, we described four soil profiles in two separate fault exposures. Soil properties are described using SCS Soil Survey methods (1992; 1999), and the soil profile descriptions are presented in Appendix A.

Based on our interpretation of the stream bank exposures and stratigraphic relations revealed by the boreholes, we excavated a fault-perpendicular trench at the Arroyo Simi site to document vertical separation of datable horizons across the fault. The trench enabled us to examine sediments covered by colluvium and inset stream terrace deposits within the logged stream bank exposures, thus allowing us to document a more complete event chronology. These fault exposures are described in more detail below.

| Table 1. Carbon 14 Ages of Stratigraphic Units at Arroyo Simi					
Sample Number	Exposure	Geologic Unit	Uncorrected Age (B.P.)	Corrected Age (cal B.P.)	Corrected Age (cal B.C./A.D.)
S-1	1997	Qp1	7260±80	8003-8177	6180 – 6005 B.C.
S-11	1997	Qt5	1470±60	1398-1508	440 – 605 A.D
S-13	1997	Qt5	1350±50	1224-1324	640 – 790 A.D
S-14	1997	Qc1	1320±50	1125-1285	6225 – 5970 B.C.
S-16	1997	Qt5	1400±50	1303-1403	410 – 645 A.D.
S-17	1997	Qp1	6880±50	7616-7716	5835 – 5635 B.C.
AS-4-5-1	2000	Qt3	1880 ± 40	1720 - 1900	230 - 50 A.D.
AS-4-6-2	2000	Qp1	6120 ± 80	6760 - 7240	4810 - 5290 B.C.
AS-T1-1a	Trench 1	Qt3	4310 ± 40	4830 - 4960	2880 - 3010 B.C.
AS-T1-10	Trench 1	Qt3	4140 ± 50	4520 - 4830	2570 - 2880 B.C.
AS-T1-11	Trench 1	Qt4	2280 ± 50	2150 - 2360	200 - 410 B.C.
AS-T1-12	Trench 1	Qt4	2200 ± 50	2060 - 2340	110 - 390 B.C.
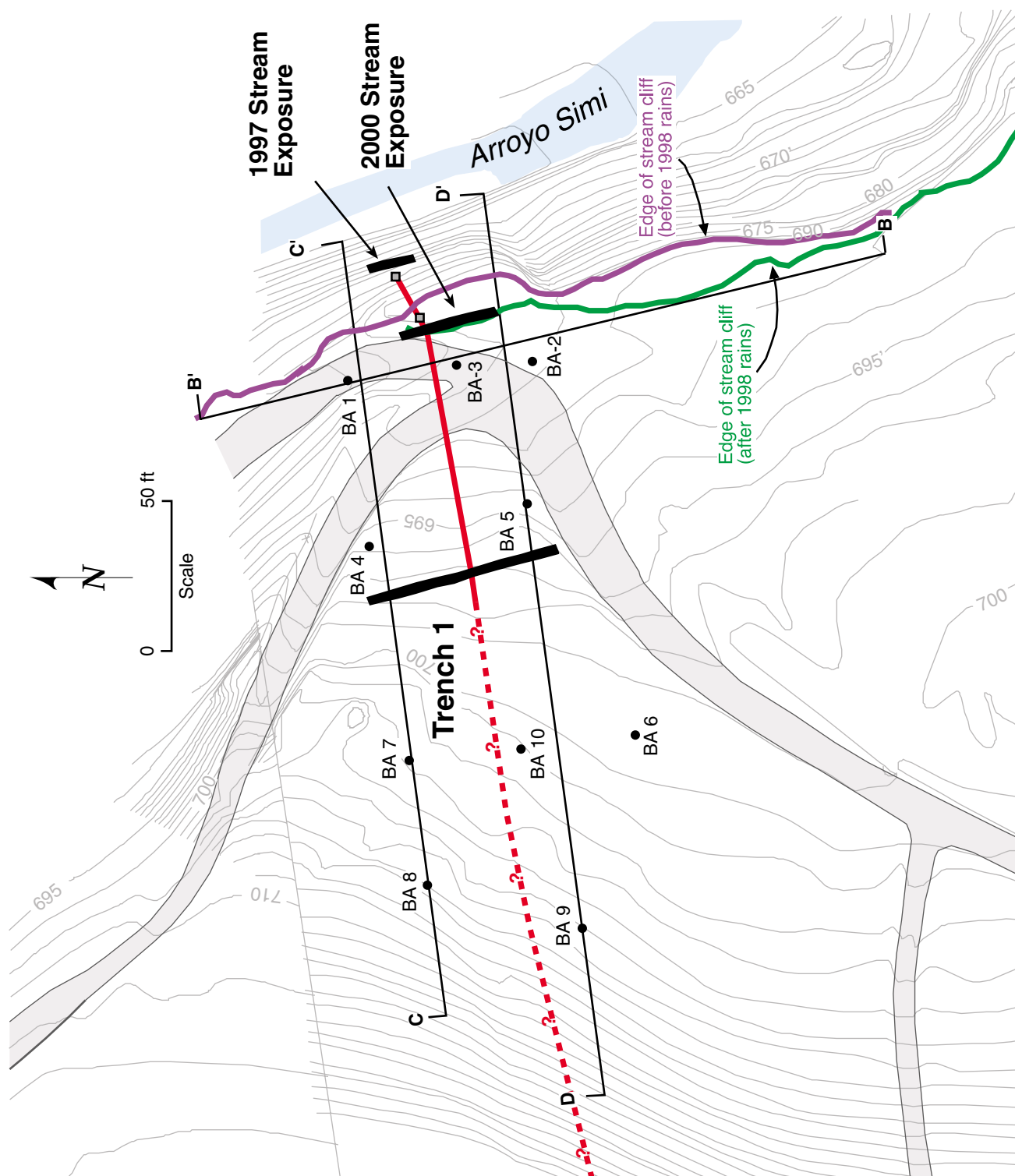
Figure 5b. Site map showing locations of paleoseismic trench, borings (BA), and stream exposures.

6.0 RESULTS

6.1 Fault Exposures
In 1997, a sequence of fluvial, colluvial, and ponded alluvial sediments extended across the Simi fault in a 50-m-long, 5- to 8-m-high, discontinuous exposure along the western stream bank of Arroyo Simi (Hitchcock et al, 1998; Figure 6). We first identified this previously undocumented fault exposure in September of 1996 as part of our Quaternary geologic mapping of surficial deposits for liquefaction hazard zonation (Hitchcock et al.,1996; Hitchcock et al., 1999).

6.1.1 1997 Arroyo Simi Exposure
At the base of the stream bank, approximately 7 m below the ground surface, clay beds were exposed in fault contact with sandstone of the Sespe Formation (Figure 7). The fault extended into overlying warped clays and inset stream channel deposits. The upper part of the exposure was obscured by a thick sequence of unfaulted colluvium. We were unable to remove colluvial deposits in the upper part of the exposure because of incipient slope failure and logistical reasons.

The fault was expressed as a N70°E striking zone of clay gouge bounded by a vertical cobble bed within the Sespe Formation on the north and clay deposits to the south (Figure 7). Distinct silty clay and sandy clay layers exposed on the inferred downthrown fault block are warped upwards near the fault. This apparent drag folding is consistent with reverse displacement on the fault.

The oldest faulted fluvial deposits within the fault exposure are in unconformable contact with underlying sandstone bedrock of the Sespe Formation and appear to have been deposited within a channel incised into the bedrock. Younger sandy fluvial deposits unconformably overlie the channel deposits. The basal fluvial unconformity of the younger deposits dips approximately 5° to the north, suggesting possible tilting. The fluvial package, and adjacent faulted clay deposits, are overlain by three distinct colluvial deposits, differentiated based on the presence of angular clasts, and slope-parallel dip. These colluvial deposits appear to be unfaulted. Subsequent streambank erosion in 1998 and 1999 removed much of the overlying colluvium and the inset stream channel south of the fault, producing a new exposure of the fault in 2000.

6.1.2 2000 Arroyo Simi Exposure
In 1998, flooding within Arroyo Simi during an especially wet El Nino winter produced massive erosion of the western stream bank. The 1997 fault exposure was destroyed and near-vertical bank failures in 1998 and 1999 exposed a stratigraphically higher geologic section in the areas previously obscured by colluvium (Figure 6). In April 2000, we cleaned the vertical face of the upper stream bank, producing a continuous exposure about four meters high and 12 meters long.

The base of the 2000 exposure revealed gray-brown to red-brown, slightly silty clay layers similar to those observed at the base of the stream bank in the 1997 exposure (Figure 8). The laminated clay layers dip moderately to steeply to the south. The clay layers are overlain by gently south-dipping late Holocene fluvial sands and silty sands deposited within an inset stream terrace. These deposits locally contain carbonate nodules, and disseminated carbonate, believed to represent a buried soil. This soil is covered by younger fluvial deposits, likely deposited as overbank sediments during a flood event, that extend to the top of the stream bank exposure. This uppermost deposit contains few to common pores and few rootlets and is interpreted as the modern A horizon. The top of the 2000 exposure consists of a plowed zone of mixed soil and fill.

Within the upper portion of the 2000 arroyo exposure, the Simi fault splits into at least two distinct strands that deform clay layers both plastically (resulting in warping) and brittlely (juxtaposing layers).

12
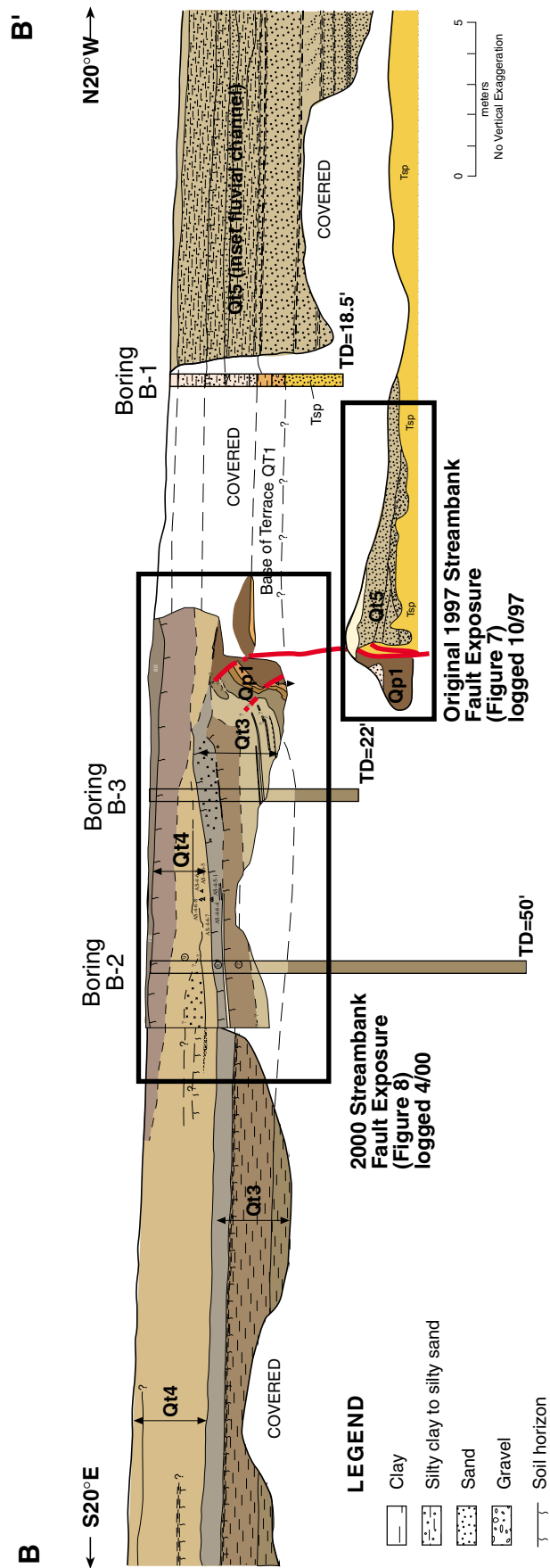
Figure 6. Cross-section B-B' along western bank of Arroyo Simi showing stream bank exposures. Cross-section is constructed from composite of natural exposures between 1997 and 2000 (covered sections are white) and bucket-auger borings B-1, B-2, and B-3. See Figure 5 for cross-section location.

13
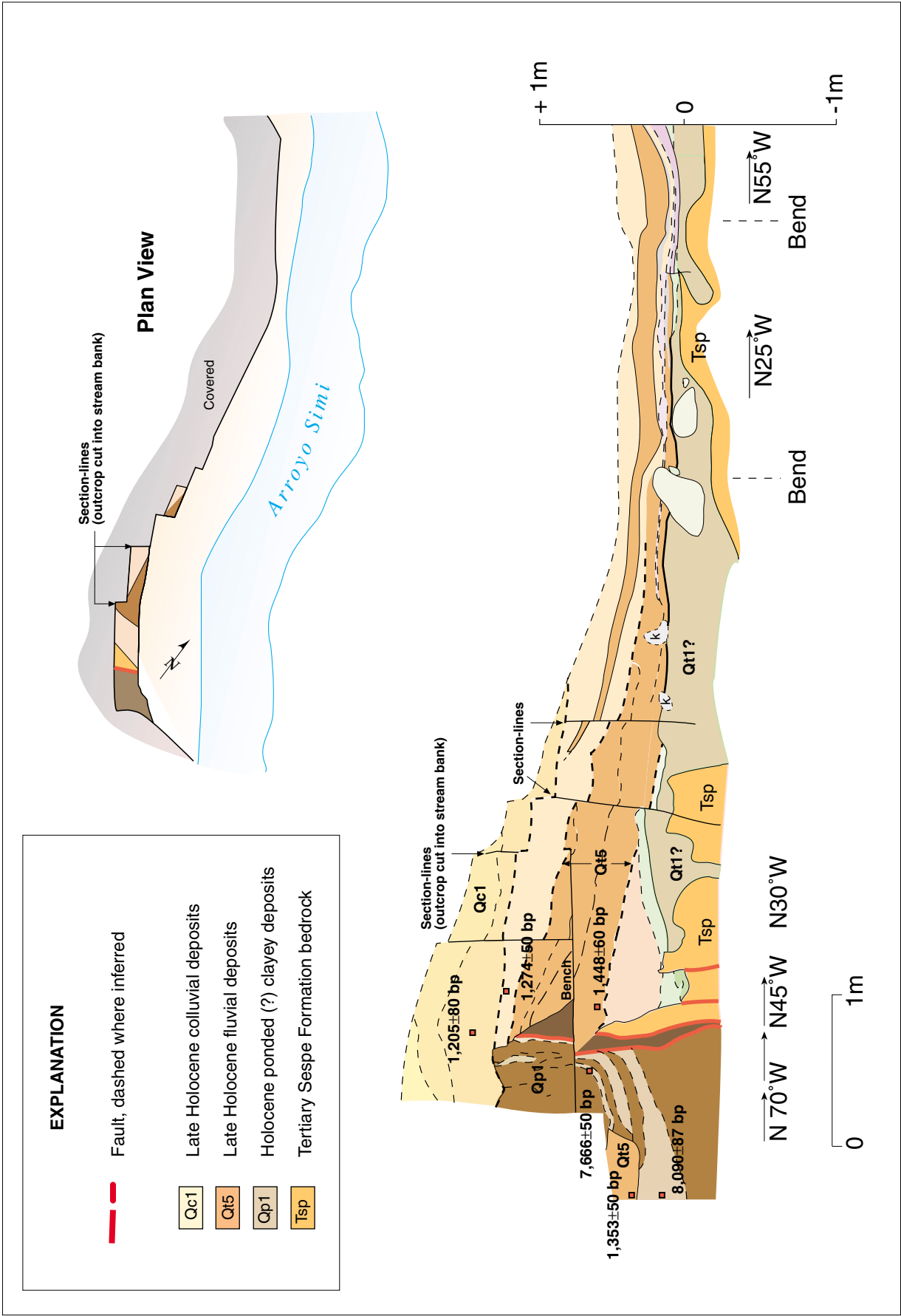
Figure 7. Plan view and section view of the 1997 Arroyo Simi fault exposure in the western streambank of Arroyo Simi.

14
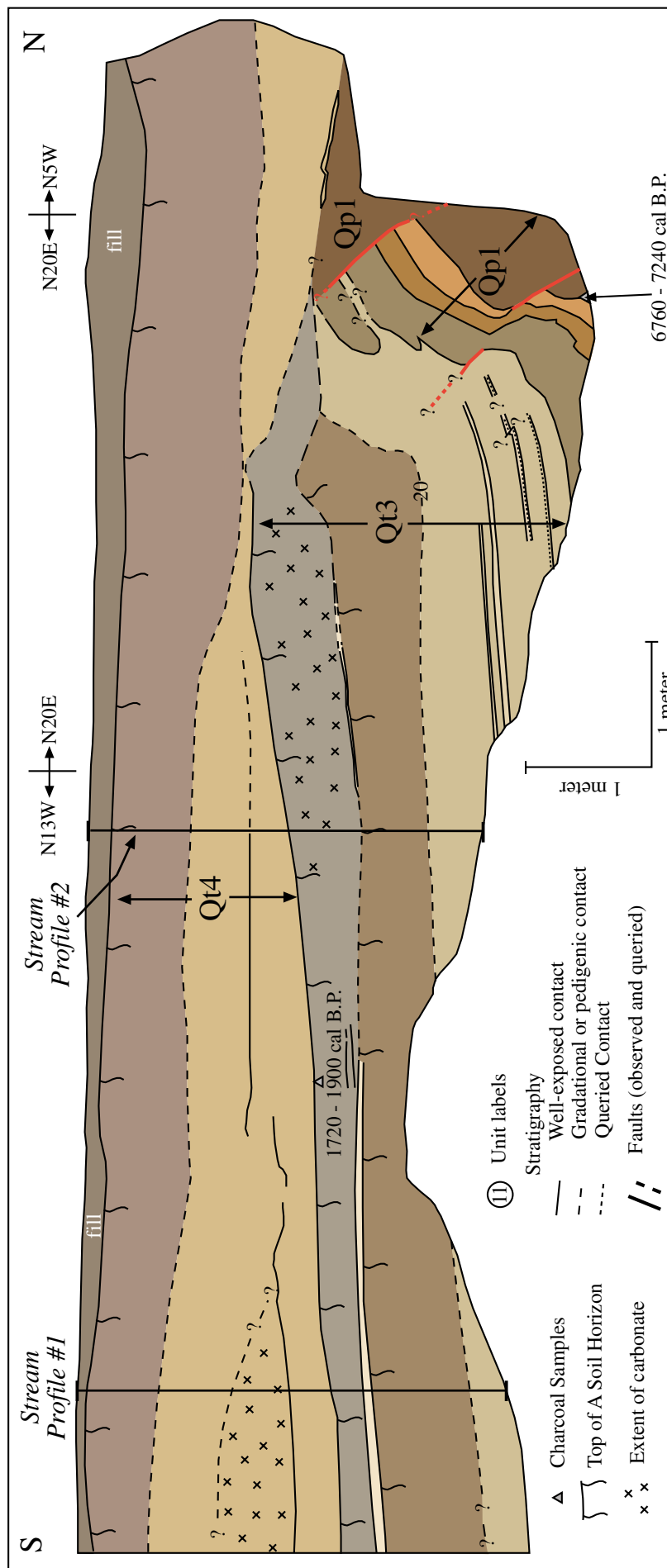
Figure 8. Simi fault exposure in western Arroyo Simi streambank, logged in April 2000.

15

6.1.3 Paleoseismic Trench Exposure 1

A paleoseismic trench was excavated to expose the main strand of the Simi fault west of the previously documented arroyo exposures. Trench 1 is about 20 m long, perpendicular to the fault, and is located approximately 26 m west of the 2000 Arroyo exposure (Figure 5b).

Trench 1 exposed gently- to moderately-south-dipping clays and fluvial silts and sands similar to those observed in the arroyo exposures (Figure 9). At the base of Trench 1, dark grayish brown massive clay on the south is juxtaposed against red-brown fine- to medium-grained, poorly-sorted clayey sand on the north. These deposits are overlain by a thin, faulted brown clay layer (Qp2). Within the trench, the fault is expressed as at least five discrete, sub-vertical fault strands. The thickness of the clay layer does not change significantly across the fault strands that cut it; however, it is absent north of the northernmost fault strand.

At the southern end of the trench, the thin, reddish-brown clay layer is overlain by a thick sequence of massive fluvial sands and silty sands. These stream terrace and overbank deposits contain pale yellow to olive brown, moderately to poorly-sorted, massive sand to silty sand with locally coarse-grained sand channels. The upper portions of the fluvial package have been overprinted by at least two episodes of soil development. The uppermost fine-grained, well-sorted silty sand contains abundant animal burrows and pores and coincides with the modern A_1 and A_2 soil horizons.

6.1.4 Borehole Data

In addition to the 1997 and 2000 fault exposures, and Trench 1, we conducted a drilling program to correlate the subsurface stratigraphy across the site and to constrain the amount of vertical separation of late Pleistocene fluvial deposits across the Simi fault. Ten 24-inch-diameter bucket auger holes were drilled, four within the hanging wall, downstream of the fault, and six within the foot wall, upstream of the fault (Figure 5b). The bucket auger borings confirm the presence of Sespe bedrock overlain by river terrace sands and gravels to the north in the hanging wall of the fault (Figure 11). We did not encounter bedrock of the Sespe formation or older terrace sands and gravels in the foot wall of the fault. Instead, borings within the foot wall revealed a thick sequence of the silty sands and clay deposits exposed in the southern end of trench 1 (Figure 12).

6.2 Site Stratigraphy

The stream, borehole, and trench exposures document massive sandstone and bedded conglomerate of the Oligocene Sespe formation (Tsp) north of the fault juxtaposed against faulted clayey alluvial deposits and overlain by faulted and unfaulted alluvial and colluvial deposits south of the fault. We divide the alluvial and colluvial deposits into three distinct groups (Figure 10): (1) silty clay Holocene pond deposits (units Qp1 and Qp2), (2) Stream terrace and overbank deposits (Qt1 through Qt5), and (3) sandy Holocene colluvium (unit Qc1).

Units are correlated between exposures based on distinct textural, stratigraphic, and pedogenic characteristics. In addition, bucket auger logs were used to correlate laterally continuous units between exposures. Cross-sections were constructed to evaluate the variability of units and correlate specific stratigraphic features used to infer slip rate. Units are described in more detail below.

6.2.1 Stream Terrace and Overbank Deposits

The oldest fluvial deposits (Qt1) are in unconformable contact with sandstone bedrock of the Sespe Formation (Tsp) and are exposed only north of the Simi fault (Figures 6 and 7). The deposits consist of coarse gravels and sandy gravel and represent channel deposits of the ancestral Arroyo Simi.
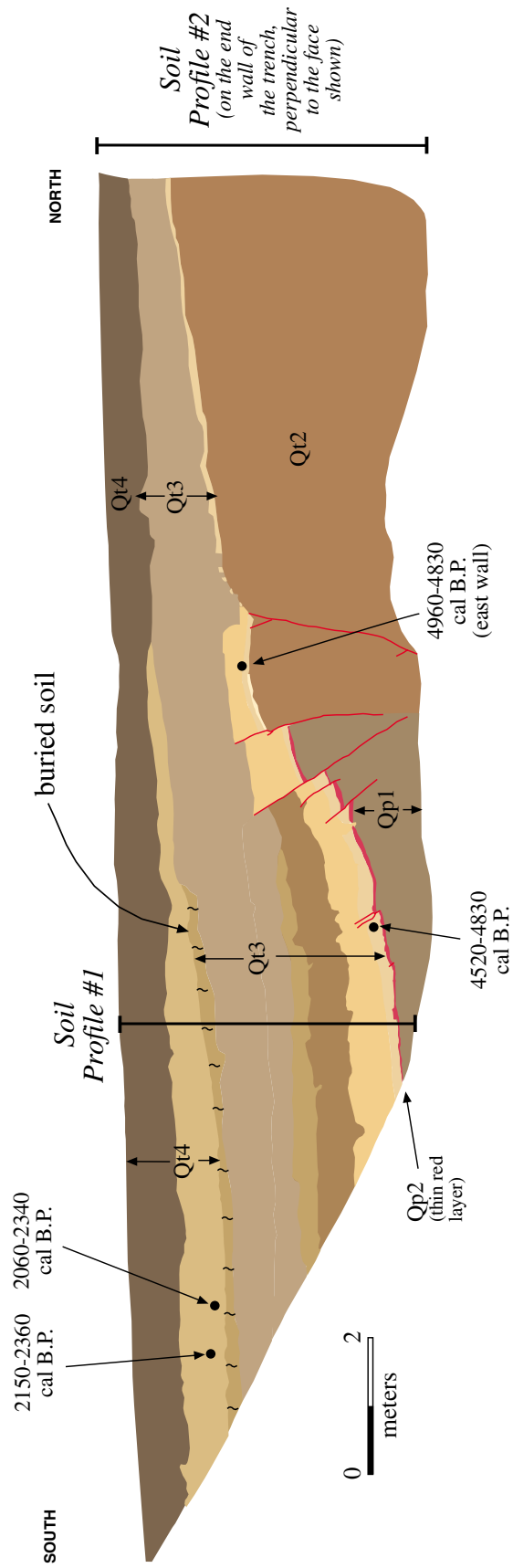
Figure 9. Log of north-south paleoseismic trench across the Simi fault. See Figure 5b for trench location.
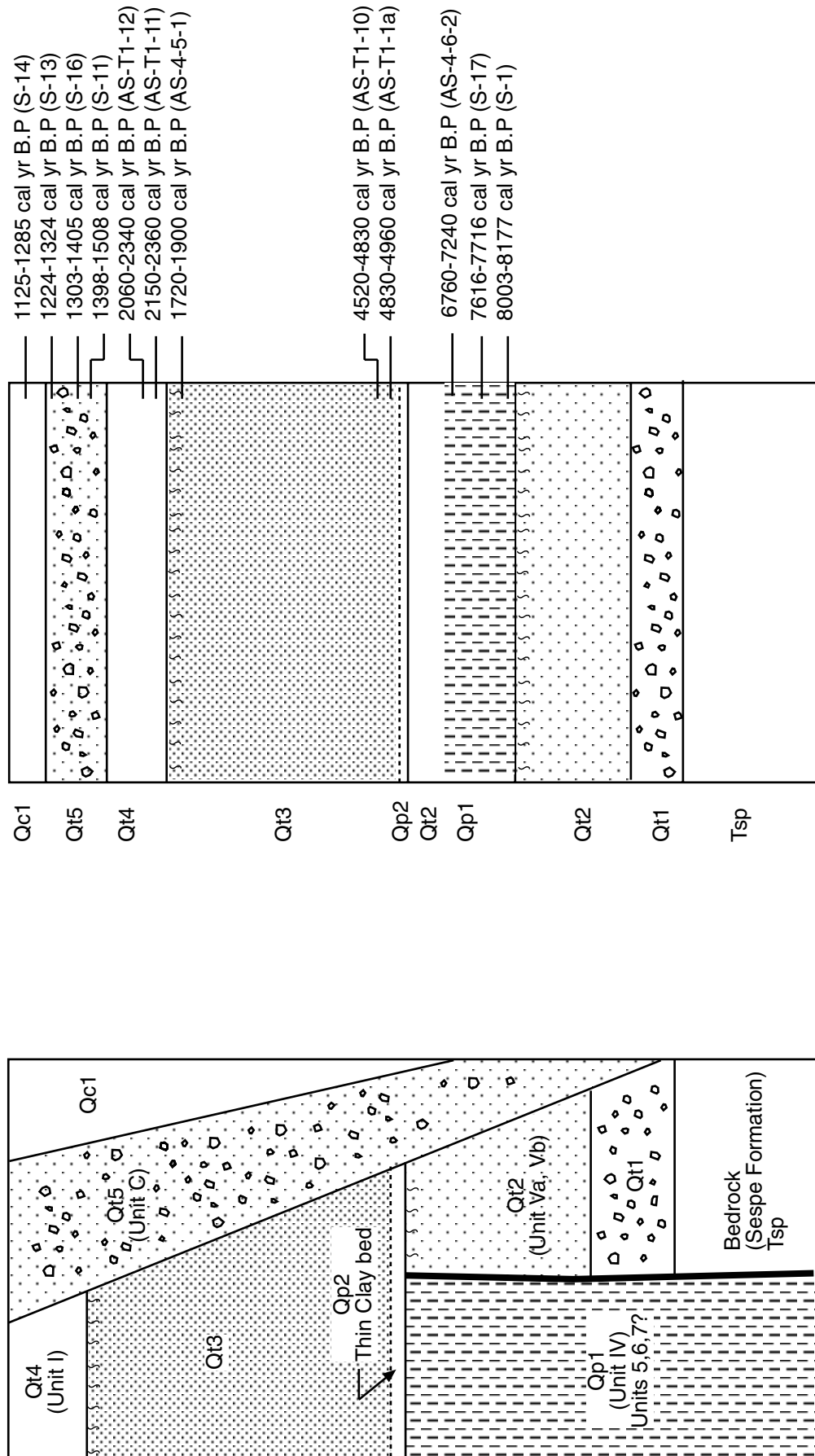
Figure 10. Idealized cross-section and stratigraphic column Radiocarbon dates are shown with sample numbers are in parentheses.

18
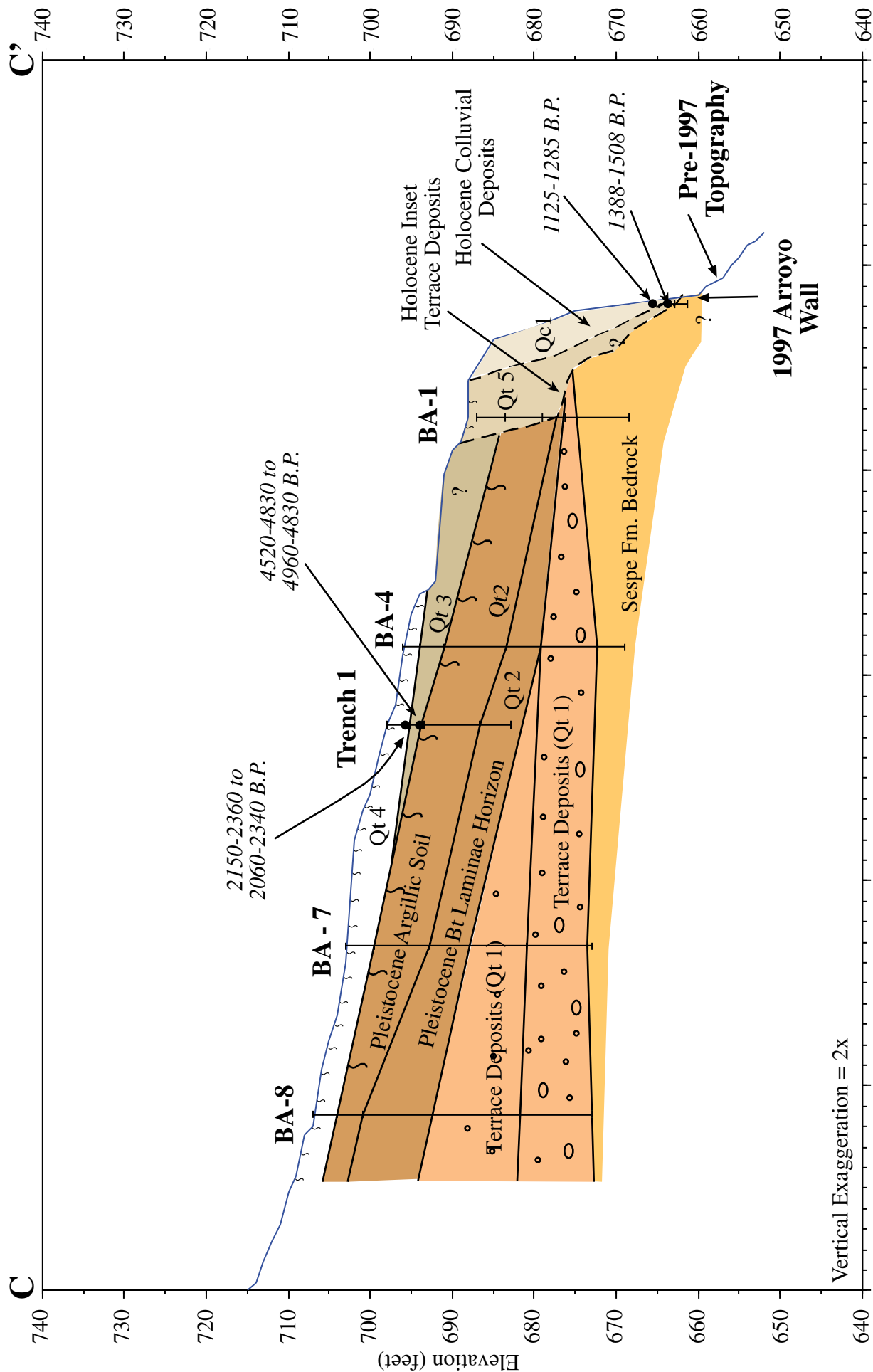
Figure 11. East-west cross-section C-C' constructed from bucket augers, trench 1, and streambank exposures north of the fault. See Figure 5 for cross section location.

19
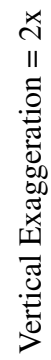
Figure 12. East-west cross-section D-D' constructed from bucket augers, trench 1, and streambank exposures south of the fault. See Figure 5 for cross section location. Cross-section is located south of the Simi fault.

20

Unit Qt2 is a fluvial unit consisting of reddish-brown, fine- to medium-grained, poorly-sorted clayey sand with abundant carbonate nodules, roots, and pores. This unit contains several well-developed argillic soil horizons, defined by clay content, soil structure, texture and other soil characteristics, and is interpreted as a Pleistocene argillic soil profile developed within fine- to medium-grained fluvial overbank deposits. Qt2 is present north of the Simi fault at the base of Trench 1 and was identified in bucket auger borings 1, 4, 7 and 8. Qt2 is in fault contact with clays of unit Qp1. The 1997 and 2000 arroyo exposures did not expose this unit. Based on cross-section C-C' (Figure 11), we believe that unit Qt2 was eroded prior to deposition of younger fluvial deposits or possibly was not exposed north of the faulted clays in the 2000 exposure.

Unit Qt3 is a fluvial unit of moderately-sorted, bedded to massive, fine- to coarse-grained silty sands. In both Trench 1 and the 2000 arroyo exposure, the base of this unit is fine-grained. However, within the 2000 arroyo exposure, Qt3 contains more clay and thin interbeds of fine-grained silty sand. The base of Qt3 in Trench 1 exhibits a coarsening upward sequence of very fine- to coarse-grained silty sand. Within Trench 1, the upper portions of Qt3 are massive; contain gray organic matter, rootlets, and pores; and have been overprinted by soil development. Qt3 locally contains carbonate nodules and disseminated carbonate, which is believed to be a modern carbonate overprint. At the north end of Trench 1, Qt3 is much thinner than to the south (0.75 cm, as opposed to 2.55 m), while in the 2000 arroyo exposure unit Qt3 is locally removed between the underlying clay (Qp1) and overlying sands (Qt4) by erosion.

Within Trench 1, fluvial sands of unit Qt4 overlie Qt3. The Qt4 fluvial sands consist of dark grayish to brown silty, fine-grained, moderately- to well-sorted silty sand. Qt4 contains abundant animal burrows and pores associated with the modern A horizon.

The youngest sandy fluvial deposits (Qt5) unconformably overlie the channel deposits observed in the 1997 arroyo exposure. The deposits consist of fine to medium-grained sand to silty sand and contain detrital charcoal that yielded corrected ages of 1388 to 1508 B.P. The basal fluvial unconformity of the younger deposits dips approximately 5° to the north, suggesting possible tilting. These deposits contain shell remnants that likely are derived from reworking of material from early or middle Miocene (Vaqueros equivalent) and middle to late Pliocene (Las Posas Fm) deposits. The terrace deposits contain shell remnants including Turritella cf. T. inezana (Conrad, 1857) similar to those collected from lower to middle Miocene "Vaqueros" deposits near Big Mountain, late Miocene to Recent *Chlamys hastata* (Sowerby, 1842), common within Pliocene and Pleistocene deposits in and around Simi Valley, late Miocene to terminal Pliocene *Patinopecten healeyi* (Arnold, 1906), common within the marine Pliocene Los Posas Formation deposits in Simi Valley, and unidentifiable oyster fragments common in both Miocene and Pliocene deposits around Simi Valley (pers. comm., L. Groves, 1997).

6.2.2 Ponded Deposits
A sequence of faulted gray-brown to reddish-brown, slightly silty clay layers, collectively called Qp1, are present south of the Simi fault at the base of all three exposures and were identified in borings 2,5,6 and 9. In trench 1, similar clay layers are faulted and juxtaposed against a late Pleistocene soil developed into older stream terrace deposits (Qt2). Detrital charcoal collected from the clays in the 2000 exposure yielded a dendro-corrected age of 6760 to 7240 B.P. which suggests that these clay layers are only slightly younger than similar, but stratigraphically lower (by about 3 m), clays within the 1997 exposure, which yielded a dendro-corrected age of 8003 to 8177 B.P. (Table 1).

Unit Qp2 overlies Qp1 and Qt2 in the trench and consists of a thin clay layer, up to 5 cm-thick. This clay layer was not observed in the arroyo exposures. Locally, the clay is reddish-brown and contains small-scale flame structures along its upper contact. It is also associated with whitish-gray clayey silt that locally contains fragments of siltstone north of the fault zone. The texture and lack

of significant sand or silt in both Qp1 and Qp2 suggests that they were deposited in a low energy, ponded environment. Similar fine-grained deposits downstream of the fault contain shells of *Gyralus parvus* (Say, 1817) & *Physa sp.*. These fossils typically are indicative of late Pleistocene or younger age and can occur within lakes with a muddy or sandy substrate that contain rooted vegetation or within permanent to subpermanent clear flowing streams (pers. comm., L. Groves, 1997)

6.2.3 Colluvial Deposits

The fluvial deposits, and adjacent clay deposits, are overlain by three distinct colluvial deposits of unit Qc1, These colluvial deposits are differentiated based on the presence of angular clasts, lack of alluvial texture, and slope-parallel dip. The colluvial deposits appeared to be unfaulted in the 1997 exposure (Figure 7).

6.2.4 Pedostratigraphic Units

Soil profiles were described within the 2000 arroyo exposure and Trench 1. Two profiles were described south of the fault in the 2000 arroyo exposure (Figure 8) and two additional soil profiles were described within Trench 1, one south of the fault, and the other at the northern end of the trench, north of the fault (Figure 9).

South of the Simi fault, we recognize at least three pedostratigraphic units, including the surficial mollic soil and two distinct buried soils. Soils are classified as entisols and are characterized by a series of four stacked mollic A horizons over non- to slightly weathered C horizon material (alluvium). The two soil profiles described in the 2000 arroyo exposure (Appendix A; Arroyo Simi exposure: Station -7 and -2), contained three stacked mollic A horizons. The soil profile described at Station 6 in the trench exposure (Figure 9), contained 4 stacked entisols because this exposure went deeper into the stratigraphic section than the 2000 arroyo exposure. The modern entisol (or surface soil), exposed in every soil profile, consists of a plowed horizon and a dark grayish brown, organic-rich A1 and A2 horizon (or mollic epipedon) over a light yellowish brown, fine loamy sand with disseminated calcium carbonate. The buried (or stacked) entisols, exposed in soil profile description locations south of the fault zone, mimic the pattern of the modern soil (organic rich A horizon over a C horizon); however these buried soils have a Holocene calcium carbonate overprint due to their present position in the subsurface.

North of the Simi fault, the soil profile described at station 2 in Trench 1 (Figure 9) consists of an entisol over a buried (exhumed) alfisol. The buried alfisol has an abrupt erosional upper boundary with the overlying C horizon, and it is characterized by a thick, yellowish brown to brown, well-developed argillic horizon with thick clay films lining pores and coating ped faces, and thin clay films bridging sand grains. The argillic horizon grades into a laminar BC horizon which contains abundant yellowish brown (10YR 5/4) clay laminae. The clay laminae represent wetting fronts that deposit clay at each season's maximum storm wetting depth. The laminar BC horizon grades into raw alluvium that consists of clean, moderately well-sorted, medium-grained sand.

6.3 Ages of Deposits

The ages of alluvial and colluvial deposits at the Arroyo Simi site are estimated based on radiocarbon analyses of twelve charcoal samples (Table 1). Charcoal samples collected from alluvial and colluvial deposits at Arroyo Simi are detrital. Detrital samples typically are older than the depositional age of an alluvial unit because they include the age of the wood at the time it was burned and the amount of residence time in the watershed before the charcoal is remobilized and deposited as alluvium. In general, we assume that the youngest of multiple detrital charcoal dates from an individual unit most closely approximates the true age of the deposit.

6.4 Fault Characteristics

The Simi fault is expressed at the base of the western stream bank of Arroyo Simi as a vertical, N70°E striking zone of clay gouge bounded by a vertical bed of cobbles within the Sespe Formation on the north and warped clay deposits to the south. Layers within the clays are warped upwards near the fault, consistent with down-to-the-south displacement across the fault (Figure 8). This apparent drag folding is consistent with a reverse component of displacement on the fault. Slickensides and mullions on the fault plane plunge N75°W with a rake of 30°E indicating a significant (~2:1 horizontal to vertical) left-lateral component of displacement. An inset stream channel of Qt5 cuts across the warped clays of Qp1 and Sespe bedrock in the 1997 arroyo exposure and is offset left-laterally an unknown amount.

Within the 2000 arroyo exposure, approximately 3m above the location of the 1997 arroyo exposure (Figure 6), the fault splays into at least two distinct strands that deform clay layers both plastically (resulting in warping) and brittlely (juxtaposing layers). The fault zone within Trench 1 consists of five fault splays with a total of 1.1 m apparent vertical brittle fault offset of unit Qp2. Faults exposed in the trench are thin, discrete planes lacking shear fabric and clay gouge, which strongly suggests that they are the result of possibly only one event.

6.5 Earthquake History

The exposed late Pleistocene and Holocene deposits at Arroyo Simi record a history of multiple late Pleistocene and Holocene earthquakes on the Simi fault. As shown on Figure 6, ponded Holocene clay deposits of unit Qp1 at least 15m thick have accumulated on the footwall of the Simi fault and have been repeatedly offset by the fault. We interpret that these clay deposits reflect repeated offset along the Simi fault, producing an upstream-facing scarp, and impoundment of the arroyo. Based on offset Holocene fluvial deposits above the clay beds, we interpret at least one and probably two distinct Holocene surface faulting events. More Holocene events are possible but could not be reliably discerned given the resolution of the stratigraphy at the site. Below, we describe the evidence for the two Holocene events, and our interpretation of the displacement per event and timing of the most recent and penultimate events. We also provide an estimate of slip rate given the stratigraphic and age constraints at the site.

6.5.1 Displacement Per Event

We have vertically reconstructed the thin red/gray clay marker bed of Qp2 in Trench 1 (Figure 13). Our reconstruction restores each block so that there is no displacement of unit Qp2 across the faults. We acknowledge that this vertical restoration omits the lateral component of slip on the fault and, thus, our estimate of displacement is a minimum. We also interpret, with uncertainty, that this restoration represents one event, due to the sharp, clean and thin fault surfaces that lack complex shear fabric. Restoration of brittle slip in the clay horizons causes the buried soil (designated by vertical lines at its upper boundary on Figure 13) below Qt4 to be restored from a dip of approximately 10° to horizontal. This suggests that the buried soil formed prior to the brittle faulting event, if the soil originally was horizontal. Because reconstruction of brittle faulting within Qp2 does not over restore the buried soil beyond horizontal, it is unlikely that more than one brittle faulting event within Qp2 occurred prior to development of the buried soil. Alternatively, the soil may have formed on the scarp created by faulting of Qp2 and thus postdates the event recorded in Qp2. This interpretation is supported by the lack of brittle faulting of this paleo-ground surface represented by the soil.

Restoration of brittle slip does not account for observed tilt in the thin, red and gray clays of Qp2 across the entire length of Trench 1 following reconstruction (Figure 13). It appears unlikely that Qp2 would have been deposited, with minimal variation in thickness, on a slope of approximately
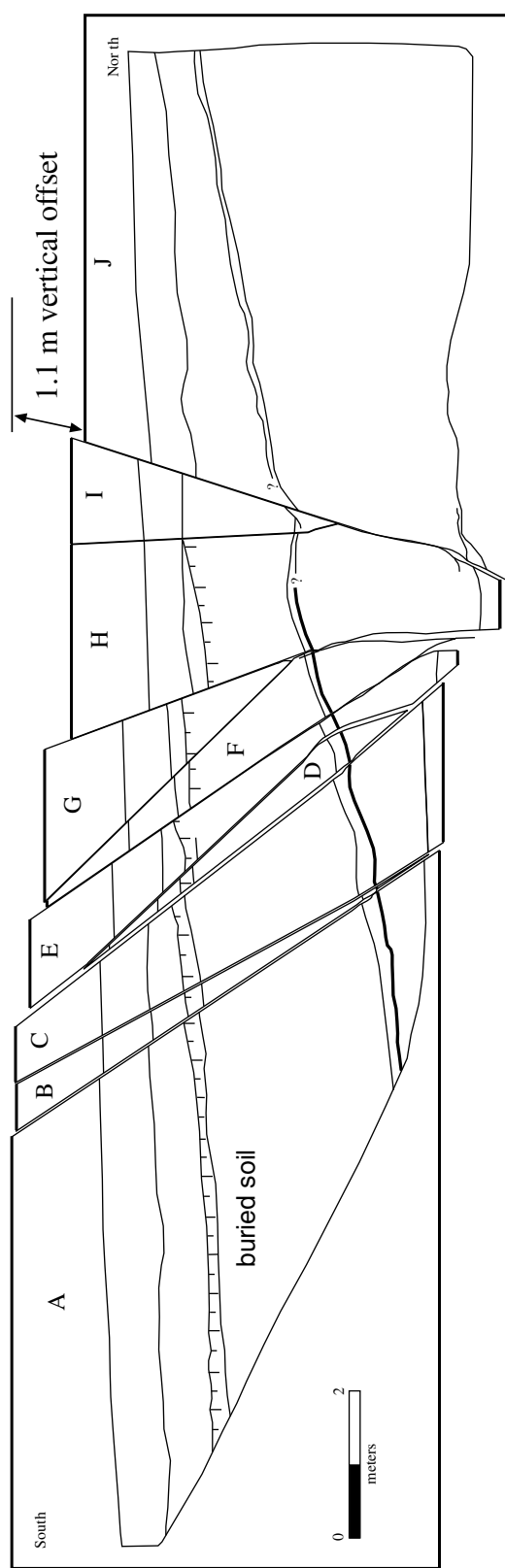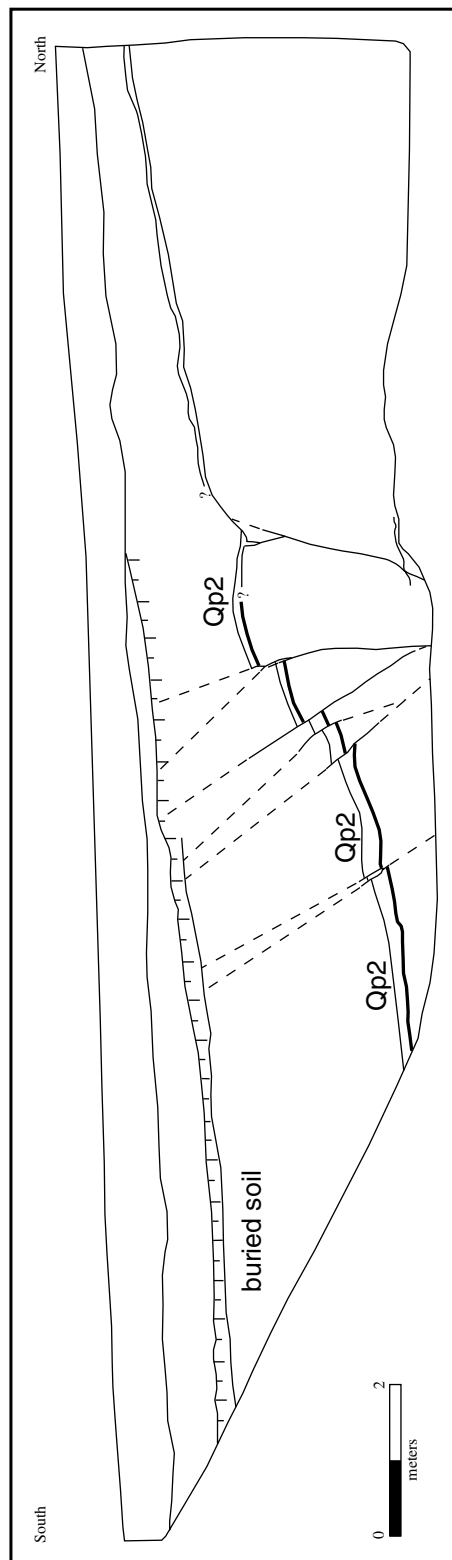
23

Figure 13. Schematic diagram showing reconstruction of fault clay marker bed (Qp2). Note that buried soil is restored to near-horizontal.

24

10°. This implies that more than one event postdates deposition of Qp2. However, as stated above, the evidence suggests that brittle faulting of Qp2 occurred in one event. An additional event tilted Qp2 but may not have produced brittle surface rupture. This prior event, or events, may be associated with the dramatic warping of clay layers within Qp1 in the 2000 arroyo exposure. Interestingly, the amount of tilting on the buried soil, approximately 10°, matches that reconstructed for Qp2. Whether the buried soil formed prior to the most recent event, or formed on a pre-existing scarp, this suggests that the similar tilting of Qp2 likely resulted from deeper fault offset on the main strand that we have documented in the exposures.

Based on our reconstruction, we obtain ~1.1 meters of vertical brittle deformation of Qp2. Using the striae recorded along the fault plane in the 1997 arroyo exposure (N75°W plunge with rake of 30°E), we obtain 2.2 meters of horizontal brittle slip and 2.6 meters of total slip. Based on published regressions correlating displacement with earthquake magnitude, this estimate of the amount of displacement is consistent with an earthquake on the order of M7 (Wells and Coppersmith, 1994).

Similarly, we use geometric reconstruction of faulted and warped clays in the 2000 arroyo exposure to develop an estimate of displacement during the penultimate event at the site (Figure 14). Approximately 1.6 m of fault-parallel dip-slip restores the base of the lower buried soil to horizontal. An additional 1.6 m (minimum) is required to restore the massive clay in Qp1 to horizontal. Based on this reconstruction, we calculate a minimum total *vertical* separation of approximately 3.2 m for Qp1. This estimate assumes that: (1) the buried soil was originally horizontal; (2) the massive clay in Qp1 was originally horizontal and tabular; and (3) that the displacement occurred in two events with an average displacement per event of 1.6m. Below we discuss evidence that we believe constrain the number and timing of events preserved within the three fault exposures.

6.5.2 Most Recent Event
Our original study of the 1997 fault exposure provided broad constraints on the timing of the most-recent events based on the youngest exposed faulted deposits (unit Qp1; 7666±50 years BP) and the age of the oldest overlying unfaulted deposits (unit Qc;1205±80 years BP; Hitchcock et al., 1998). Although we believed at the time that inset stream channel deposits of unit Qt5 present on both sides of the fault in the 1997 exposure likely were faulted, we did not have sufficient information to document fault offset.

Subsequent erosion of the Arroyo Simi stream bank removed the channel deposits south of the fault and exposed channel deposits of unit Qt5 north of the fault that are deeply channeled into Sespe bedrock. The geometry of the newly exposed channel deposits indicates that these deposits are in fact faulted across the Simi fault in an oblique left-lateral, reverse sense. This interpretation constrains the timing of the most recent event on the Simi fault between about 1,120 to 1,285 BP (the age of the unfaulted colluvium; unit Qc) and about 1,300 to 1,500 BP (the age of the faulted channel deposits, unit Qt5).

Restoration of brittle slip in the Qp1 and Qp2 clay horizons in Trench 1 and the 2000 arroyo exposure causes prominent buried soils to be restored to horizontal (Figures 13 and 14). This suggests that the buried soils formed prior to the most recent brittle faulting event, if the soil originally was horizontal. Alternatively, the soil could have formed on a pre-existing scarp and therefore postdates the event recorded within Qp2 in Trench 1. This interpretation is supported by specifically an inferred internal horizontal contact within Qt4, observed in the 2000 exposure, that suggests that this unit is not tilted but rather formed by onlap onto pre-existing topography represented by the underlying, south-dipping buried soil (Figure 8). Thus, although the base of

25

unrestored

1.6 m along fault plane

base of soil restored

3.2 m total

older scarp restored

tilted 37°

1720 - 1900 cal B.P

6760 - 7240 cal B.P.

1 meter

1 meter
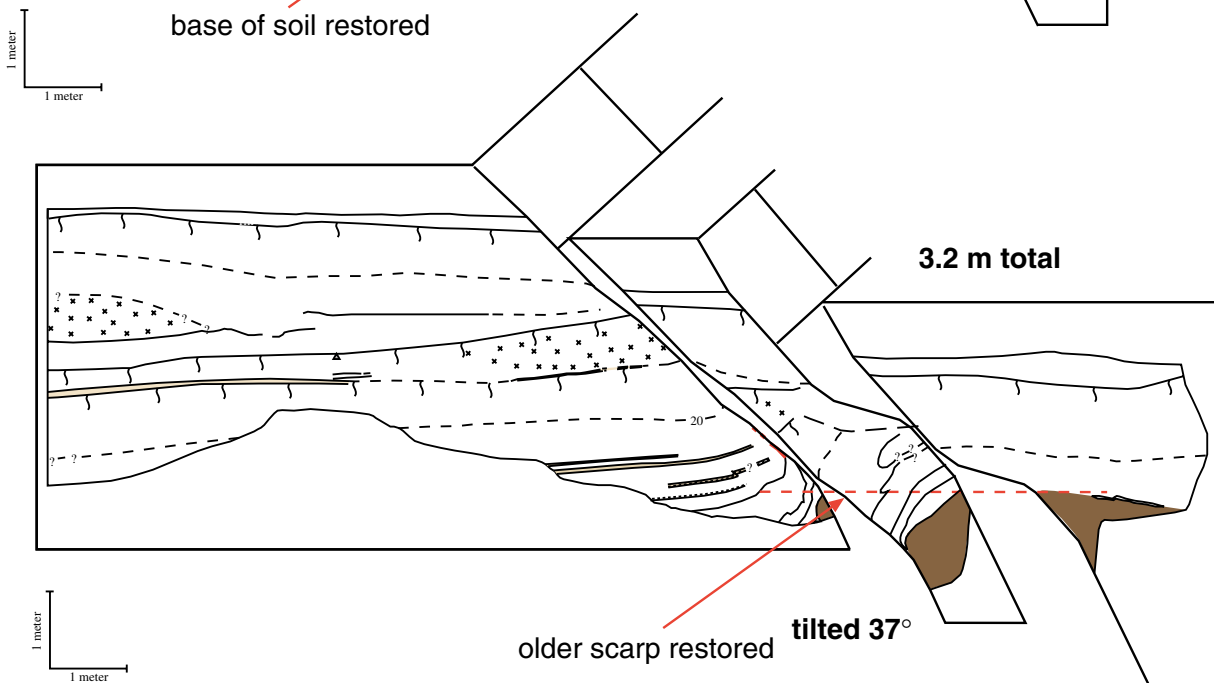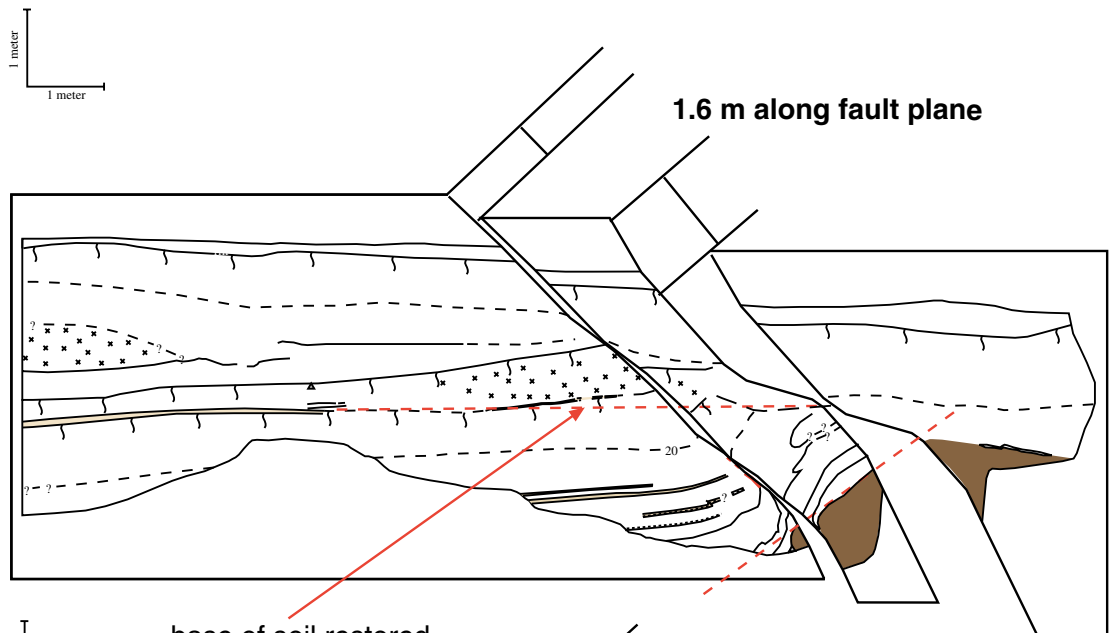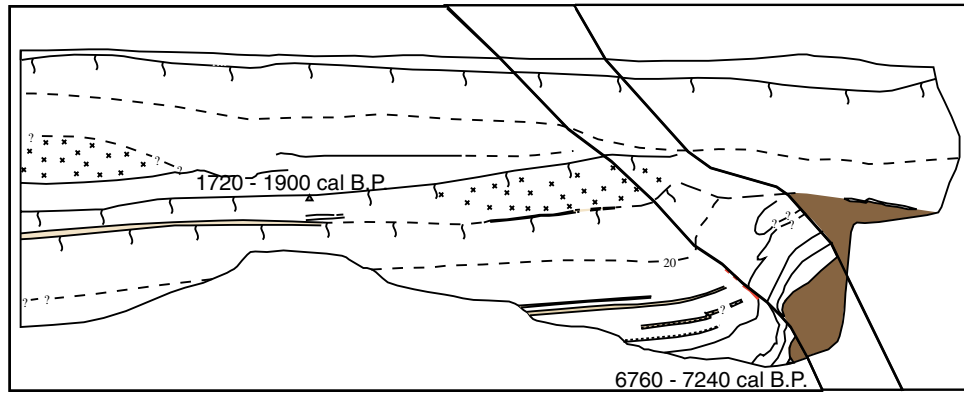
1 meter

1 meter

1 meter

1 meter

20

20

20

Figure 14. Schematic diagram showing reconstruction of faulted clay layers in 2000 arroyo exposure.

26

Qt4 appears tilted, Qt4 may not have been tectonically deformed by the most recent event. Because the date obtained from the soil in the 2000 arroyo exposure closely matches that obtained from the base of Qt4 in Trench 1, the interpretation that Qt4 is unfaulted suggests that the underlying soil of similar age may also not be faulted but rather may have formed on a pre-existing scarp. If this alternative interpretation is correct, the timing of the most recent event is constrained between the age of the faulted Qp2 unit in Trench 1 (4520 to 4960 BP) and dates obtained within the soil in the 2000 exposure (1720 to 1900 BP) and within Qt4, above the buried soil, in Trench 1 (2060 to 2360 BP). This interpretation requires that the apparent offset channel across the fault in the 1997 exposure is not the result of faulting, but rather an abrupt meander bend in the channel.

In summary, our preferred interpretation is that the MRE is constrained about 1,120 to 1,285 BP (the age of the unfaulted colluvium) and about 1,300 to 1,500 BP (the age of the faulted channel). However, based on an alternative interpretation of the stratigraphic record, the most recent event may be more broadly constrained between the age of a buried soil in Trench 1 and the 2000 exposure (1720 to 2360 BP) and the age of the faulted Qp2 unit in Trench 1 (4520 to 4960 BP).

6.5.3 Penultimate Event
The main vertical strand in Trench 1 juxtaposes two very different units, unit Qt2 on the north against unit Qp1 on the south. However, unit Qp2 is draped across both units with minimal change in its thickness across the fault. These relationships suggest that the vertical strand of the Simi fault likely has produced several earthquakes prior to the deposition of unit Qp2, between 6760 – 7240 B.P. and 4960 – 4830 B.P. However, as stated above, the sharp, clean fault strands that offset Qp2 lack complex shear fabric and appear to be the result of a single event.

Therefore, we interpret that the penultimate event probably did not deform the unit Qp2 (4,500 to 5,000 BP), unless it produced the overall tilt to the south of the unit present after reconstruction (Figure 13). If an event prior to the most recent event had faulted the Qp2 clay, there should still be apparent near-fault warping after reconstruction of brittle slip similar to that of the older clays seen in the 2000 arroyo exposure after similar restoration (Figure 14). In short, there should be remnants of an earlier scarp preserved by the Qp2 clay layer, detectable in the reconstruction.

Similarly, reconstruction of the faulting in the 2000 arroyo, about 1.6 m of dip separation restores the base of the 1720-1900 years-old tilted/warped buried soil to horizontal. However, this amount of reconstruction does not restore the underlying warped 6700 to 7200 year-old clay beds . These beds still are warped and appear to preserve a buried scarp. An additional 1.6 m of fault-parallel slip is required to restore these beds. This slip estimate is a minimum because the upper portion of the unit Qp1 clays on the hanging wall north of the fault are scoured by younger inset terrace deposits. Thus, the penultimate event likely postdates the 6700 to 7200 year-old Qp1 clays exposed in the 2000 arroyo exposure but predates the 4,500 to 5,000 year old thin clay (unit Qp2) that crosses the fault in Trench 1. This would also explain the significantly greater deformation of clays (warping/folding) observed in the arroyo exposures than the Qp2 clay in Trench 1.

6.5.4 Holocene Slip Rate
We estimate the Holocene net slip rate on the fault using vertical separation of dated alluvial beds and slickensides documented in the 1997 exposure as a proxy for the net slip vector. Averaging the displacements associated with the two Holocene events observed in the trench and steam bank exposures over the elapsed time since the penultimate event (about 3.2 m over 6,700 to 7,200 years) results in a minimum dip slip rate of about 0.4 to 0.5 mm/yr. Based on the slip vector derived from the slickensides and mullions (30 degree rake), we obtain an overall fault slip rate of 0.9 to 0.95 mm/yr. However, the slip rate may be even higher based on the observation that the penultimate event postdates the 6700 to 7200 year old clays exposed in the 2000 exposures but predates the 4,500 to 5,000 year old clay marker bed that crosses the fault in Trench 1. If we assume that the

penultimate event occurred prior to deposition of unit Qp2, 4,500 to 5,000 years ago, we obtain a dip slip rate of 0.6 to 0.7 mm/yr and an overall slip rate of about 1.3 to 1.4 mm/yr.

We do not know how representative the Holocene slip rate, based on only two events, is of the longer-term Quaternary slip rate. The few available constraints on longer-term activity suggest rates similar to the inferred Holocene rate. Yeats (1983) cited 600 feet (163 m) of late Quaternary vertical separation across the Simi fault based on correlation of the base of post-Saugus terrace deposits capping bedrock within the Simi Anticline north of the fault to the buried bedrock base of the valley. Assuming a dip on the fault of 65°, and an age for post-Saugus gravels of 200 ka (after Gonzalez and Rockwell, 1991) to 500 ka (Levi and Yeats, 1993), we estimate a late Quaternary dip slip rate of approximately 0.4 to 0.9 mm/yr. However, based on our previous examination of borehole data (Hitchcock et al. 1996, 1999), we believe that the terrace deposits capping bedrock north of the fault possibly are correlative to the buried contact between fine-grained sediments and underlying coarser, older deposits. This correlation yields a dip slip of 350 feet (107 m) and an estimated late Quaternary vertical separation rate of 0.2 to 0.6 mm/yr for the Simi fault. If we apply a component of left-lateral slip to these rates of vertical separation, the net long-term slip rate on the fault ranges from about 1 to 1.5 mm/yr.

In summary, using our reconstruction of brittle slip in Trench 1 and the 2000 arroyo exposure, we obtain a Holocene slip rate that incorporates two events over the past ~7,000 years. This minimum total slip rate is 0.9 to 1.4 mm/yr and may be higher because we have lost some of the record on the north side of the 2000 arroyo exposure. Alternatively, we derive a slightly lower total slip rate of 0.7±0.2 mm/yr from the average per-event vertical separation of 1.5±0.1m, determined from our fault slip reconstructions, and an interseismic interval between the two events of about 3,100 to 5,900 years.

7.0 DISCUSSION

The role of the Simi-Santa Rosa fault within the regional tectonic regime is poorly understood. The Simi-Santa Rosa fault zone is within the hanging wall of the larger Oak Ridge fault system (Huftile and Yeats, 1994). However, it is unclear how the Simi fault and associated faults are related to the Oak Ridge fault system. Specifically, are the events documented on the Simi fault related to large earthquakes on the Oak Ridge fault system?

7.1 Kinematics and Relationship to Other Faults
Currently, two competing models have been proposed to explain how strain is being accommodated within the southwestern Transverse Ranges. Walls et al. (1998) proposed that north-south shortening is coupled with east-west lengthening, accommodated at least in part by a significant component of sinestral slip on the regional fault systems. Alternatively, Argus et al. (1999), argue that north-south shortening is accommodated mainly by vertical crustal thickening via reverse faulting.

Our data show evidence of both reverse and sinistral displacement on the Simi fault. Slickensides, mullions, and left-lateral offset of channel deposits are consistent with available geomorphic and structural evidence that show a significant component of sinistral slip on the Simi fault (i.e. Yeats, 1983; Hanson, 1981). It is likely that regional strain is accommodated by both north-south shortening in the hanging wall of the Simi fault, and other major thrust fault systems, and by east-west lengthening via lateral displacement along the sub-vertical faults.

Our estimate of slip rate on the Simi fault is a third of the 3-6 mm/yr slip rate estimated on the Oak Ridge fault (Yeats, 1998; Dolan et al, 1995). Regional structural cross-sections (Huftile and Yeats, 1994) indicate that the Simi-Santa Rosa fault system forms a back thrust within the hanging wall of

the larger Oak Ridge fault. Although the timing of events on the Oak Ridge fault currently is poorly constrained, comparison of the timing of events on the Simi fault to that on the Oak Ridge fault may confirm a temporal connection between events on the apparently connected faults.

7.2 Size and Frequency of Earthquakes on the Simi-Santa Rosa Fault System

Based on empirical relations of Wells and Coppersmith (1994), the amount of vertical offset that we estimate across the Simi fault likely requires rupture of the entire Simi-Santa Rosa fault zone, including the Springville and Camarillo faults at the western end of the fault zone. Gonzalez and Rockwell (1991) used buried soil horizons to estimate vertical displacement per event of 0.6 to 1.1m on the Springville fault, at the western end of the Simi-Santa Rosa fault system (Figure 1). In addition, based on the soil development within faulted deposits, the most recent event on the Springville fault likely occurred less than 1000 to 2000 years ago (Gonzalez and Rockwell, 1991). Although poorly constrained, these estimates are consistent with the timing and displacement per event of the most recent event we document at Arroyo Simi.

7.3 Implications for Seismic Hazard Assessment in the Ventura Basin

The Simi-Santa Rosa fault zone appears to be capable of producing earthquakes as large as M7, based on the inferred amount of displacement per event that we document on the Simi fault (Wells and Coppersmith, 1994). Strain likely has been accumulating on the Simi fault since the time of the most recent earthquake at least 1,125 to 1,508 years BP.

Currently the Simi-Santa Rosa fault zone has been placed within a special study zone by the State of California (Treiman, 1999). However, pre-existing residential and commercial structures are located within the AP zone and, in some cases, atop active strands of the Simi-Santa Rosa fault zone. In addition, extensive liquefaction-related damage in Simi Valley and elsewhere in Ventura County during the 1994 Northridge earthquake clearly demonstrates the vulnerability of the region to effects from strong ground shaking. Large-scale development of the Oxnard Plain and Santa Clara River Valley has led to artificial filling and urbanization of large tracts of land. These areas are underlain, in large part, by young unconsolidated stream deposits that may be particularly susceptible to liquefaction (Hitchcock et al., 2000). Thus, an earthquake on the Simi-Santa Rosa fault zone likely would result in significant widespread damage and must be considered in future planning scenarios within Ventura County.

8.0 CONCLUSIONS

Results from our paleoseismic investigation at Arroyo Simi provide data on the activity and sense of slip of the Simi fault. The Simi fault accommodates oblique, left-lateral-reverse slip based on documentation of warped and offset bedding, slickensides on the main fault plane, and left-lateral offset of an inset fluvial channel across the fault. The most recent event on the fault occurred between about 1,120 to 1,285 BP (the age of unfaulted colluvial deposits) and 4520 to 4960 BP (the age of the faulted Qp2 unit in Trench 1). Alternatively, the most recent event may have occurred between 2060 to 2360 BP (the age of a buried soil) and 4520 to 4960 BP. Based on our preferred interpretation of the stratigraphic record, the most recent event may be more narrowly constrained between 1,120 to 1,285 and about 1,300 to 1,500 BP (the age of an apparently faulted stream channel). The penultimate event probably occurred between 6700 to 7200 BP (based on faulted clays exposed in the 1997 and 2000 arroyo exposure) and 4,500 to 5,000 BP (based on reconstruction of the Qp2 clay marker bed in Trench 1). These events likely were associated with vertical displacements on the order of about 1 to 1.5 m.

The results of this study show that the Simi fault plays a significant role in accommodating strain within the Transverse Ranges. The Simi fault, and entire Simi-Santa Rosa fault zone, should be considered an active seismogenic source in regional seismic hazard assessments.

9.0 ACKNOWLEDGEMENTS

10.0 REFERENCES

Argus, D.F., Heflin, M.B., Donnellan, A., Webb, F.H., Dong, D., Hurst, K.J., Jefferson, D.C., Lyzenga, G.A., Watkins, M., and Zumberger, J.G., 1999, Shortening and thickening of metropolitan Los Angeles measured and inferred using geodesy: Geology, v. 27, p. 703-706.

Birkeland, P., 1984, Soils and Geomorphology, Oxford University Press, New York, p. 357.

Blake, T. F., 1991, Synopsis of the character and recency of faulting along the Simi-Santa Rosa fault system; *in* T F. Blake and R. A. Larson, eds., Engineering geology along the Simi-Santa Rosa fault system, p. 96-118.

Davis, T.L., and Namson, J.S., 1994, A balanced cross-section of the 1994 Northridge earthquake, southern California: Nature, v. 372, p. 167-169.

Dibblee, T.W. Jr., 1991, Geology of the Simi fault zone; *in* T F. Blake and R. A. Larson, eds., Engineering geology along the Simi-Santa Rosa fault system, p. 157-163.

Dolan, J.F., Sieh, K., Rockwell, T.K., Yeats, R.S., Shaw, J., Suppe, J., Huftile, G.J., and Gath, E.M., 1995, Prospects for larger or more frequent earthquakes in the LA Metro. Region: Science, v. 267, p. 199-204.

Dolan, J.F., Sieh, K., and Rockwell, T.K., 2000, Late Quaternary activity and seismic potential of the Santa Monica fault system, Los Angeles, California: Geological Society of America Bulletin v.112, n. 10, p. 1559–1581.

Edwards, R.D., Rabey, D.F., and Kover, R.W., 1969, Soil Survey of the Ventura Area, California, Soil Conservation Service, U.S. Department of Agriculture, Washington D.C., p. 104.

Gonzalez, T., and T. K. Rockwell, 1991, Holocene activity of the Springville fault in Camarillo; *in* T F. Blake and R. A. Larson, eds., Engineering geology along the Simi-Santa Rosa fault system, Ventura Co., CA, p. 369-383.

Hanson, D. W., 1981, Surface and subsurface geology of the Simi Valley area, Ventura County, California: unpublished M.S. Thesis, Oregon State University, 112 p.

Hitchcock, C.S., Loyd, R.C., and W.D. Haydon, 1996, Liquefaction susceptibility and hazard zone mapping, Simi Valley, California [abs]: Eos, Vol. 77, No. 46, p. F510.

Hitchcock, C.S., Loyd, R.C., and Haydon, W.D., 1999, Mapping liquefaction hazards in Simi Valley, Ventura County, California: *Environmental & Engineering Geoscience*, Vol. V, No. 4, p. 441-458.

Hitchcock, C.S., Treiman, J.A., Lettis, W.R., and Simpson, G.D., 1998, Paleoseismic investigation for the Simi fault at Arroyo Simi, Simi Valley, California: Geological Society of America Abstracts with Programs [abs], Vol. 30, No. 5., p. 19.

Huftile, G.J., and Yeats, R.S., 1996, Deformation rates across the Placerita (Northridge Mw=6.7 Aftershock zone) and Hopper Canyon segments of the western Transverse Ranges deformation belt: Seismological Society of America Bulletin, v. 86, part B, p. 3-18.

Leighton and Associates, 1972, Groundwater study (Phase II) of East and West Basin areas, City of Simi Valley, Ventura County, California: unpublished report, 18 p.

Lettis, W.R., and Hanson, K.L., 1991, Crustal strain partioning: Implications for seismic hazard assessment in western California: Geology, v. 19, p.559-562.

Levi, S., and Yeats, R.S. ,1993, Paleomagnetic constraints on the initiation of uplift on the Santa Susana fault, western transverse ranges, California, Tectonics, v. 12, No. 2, pp.688-702.

Petersen, M.D., Cramer, C., Bryant, W.A., Reichle, M.S., and T.R. Toppozada, 1996, Preliminary Seismic Hazard assessment for Los Angeles, Ventura, and Orange Counties: BSSA, Vol. 86, No., Part B., p. S247-S261.

Petersen, M. D. and Wesnousky, S.G., 1994, Fault slip rates and earthquake histories for active faults in southern California. Bulletin of the Seismological Society of America, Vol. 84, No. 5, pp. 1608-1649.

Rockwell, T., 1982, Soil chronology, geology, and neotectonics of the north-central Ventura Basin, California: Ph.D. Dissertation, University of California, Santa Barbara, p. 96.

Smiley, T.L., Bryson, R.A., King, J.E, Kukla, G.J., and Smith, G.I., 1991, Quaternary Paleoclimates, *in* Morrizon, R.B., ed., Quaternary nonglacial geology; Conterminous U.S.: Boulder, Colorado, Geological Society of America, Geology of North America, v. K-2.

Soil Survey Staff, 1992, Keys to Soil Taxonomy: 5th edition, SMSS technical monograph 19, Pocahontas Press, Inc., Blacksberg, Virginia, p. 556.

Soil Survey Staff, 1999, Keys to Soil Taxonomy: 7th edition, SMSS technical monograph 19, Pocahontas Press, Inc., Blacksberg, Virginia, p. 556.

Sorlien, C.C., Gratier, J.-P., Luyendyk, B.P., Hornafius, J.S., and Hopps, T.E., 2000, Map restoration of folded and faulted strata across the Oak Ridge fault, onshore and offshore Ventura basin, California: Geolgoical Society of America Bulletin, v. 112, p. 1080-1090.

Swift, C.A., Renger, S.A., Barrett, M.A., and Thams, P.L., 1991, Exploratory trenching of the Simi-Santa Rosa fault zone in the city of Simi Valley, California; *in* T F. Blake and R. A. Larson, eds., Engineering geology along the Simi-Santa Rosa fault system, p. 157-163.

Treiman, J.A., 1999, The Simi-Santa Rosa fault: California Division of Mines and Geology fault evaluation report FER : Sacramento, California Division of Mines and Geology.

Walls, C., Rockwell, T., Mueller, K., Bock, Y., Williams, S., Pfanner, J., Dolan, J., and Fang, P., 1998, Escape tectonics the Los Angeles metropolitan region and implications for seismic risk: nature, v. 394, p. 356-360.

Webber, F.H., Jr., Cleveland, G.B., Kahle, J.E., Kiessling, E.W., Miller, R.V., Mills, M.F., Morton, D.M., and Cilweck, B.A., 1973, Geology and Mineral resources study of southern Ventura County, California: California Division of Mines and Geology Preliminary Report 14, 102 p.

Wells, D., and Coppersmith, K., 1995, New empirical relationships among magnitude, rupture length, rupture width, rupture area, and surface displacement: Seismological Society of America Bulletin, v. 84, p. 974-1002.

Working Group on California Earthquake Probabilities, 1995, Seismic hazards in southern California: Probable earthquakes, 1994 to 2024: Seismological Society of America Bulletin, v. 85, p. 379-429.

Yeats, R. S., 1983, Simi: A structural essay: in Cenozoic geology of the Simi Valley area, southern California: in Cenozoic Geology of the Simi Valley area, R. L. Squires and M. V. Filewicz *eds.*, SEPM Field Trip Guide, p. 233-240., California: *Environmental and Engineering Geocience*, Vol. V, No. 4, p. 419-439.

Appendix A.
Soil Descriptions at the Arroyo Simi Site.

We described four soil profiles in two separate exposures across the site. The soil properties were described according to SCS Soil Survey Staff (1992 and 1999) methods, and the soil profile descriptions are presented herein. Two of the soil profiles were described on a vertical exposure along the west bank of Arroyo Simi at the 2000 arroyo exposure, at stations –7 and –2, both of which are located south of the fault at this locality (Figure X). The other two soil profiles were described within the excavated Trench 1 exposure at station 6 south of the fault, and the other at the northern end of Trench 1 (no station number), north of the fault. The properties of the soil profiles described have relatively minor variations along and parallel to the fault zone, but have sharply contrasting differences across the fault zone.

South of the Simi fault, the soils are classified as entisols and are characterized by a series of stacked mollic A horizons over non- to slightly weathered C horizon material (alluvium). Both of the soil profiles described in the arroyo wall exposure contained 3 stacked entisols. The soil profile described at station 6 in the trench exposure contained 4 stacked entisols because this exposure went deeper into the stratigraphic section than the 2000 arroyo exposure. The modern entisol (or surface soil), exposed in every soil profile description location across the fault zone, consists of a plowed horizon and a dark grayish brown, organic rich A1 and A2 horizon (or mollic epipedon) over a light yellowish brown, fine loamy sand with disseminated calcium carbonate. The buried (or stacked) entisols, exposed in soil profile description locations south of the fault zone only, mimic the pattern of the modern soil (organic rich A horizon over a C horizon), however these buried soils have a Holocene calcium carbonate overprint due to their position in the subsurface. The soil described at station –2 in the Arroyo exposure is problematic in that it has a higher concentration of calcium carbonate and more diffuse soil horizon boundaries. This difference may be attributed to this profile's close proximity to the fault zone (Figure 8). The diffuse boundaries and higher calcium carbonate concentrations could be caused by groundwater fluctuations near the fault and/or during times of tectonic activity. The buried soil profile boundaries can be traced from the western edge of Arroyo Simi to the west across the entire southern portion of the study area.

There was one soil profile described north of the fault zone in the trench exposure, and it is classified as an entisol over a buried (exhumed) alfisol. The surface soil (or entisol) is identical to those exposed and described south of the fault. The buried alfisol has an abrupt erosional upper boundary with the overlying C horizon, and it is characterized by a thick, yellowish brown to brown, well-developed argillic horizon with thick clay films lining pores and coating ped faces, and thin clay films bridging sand grains. The argillic horizon grades into a laminar BC horizon which contains abundant yellowish brown (10YR 5/4) clay laminae, which represent wetting fronts that deposit clay at each season's maximum storm wetting depth. The laminar BC horizon grades into raw alluvium that consists of clean, moderately well-sorted, medium-grained sand.

The surficial entisol that mantels the entire study site is relatively young and not well developed. Minimal time is required (100's of years) to develop an A horizon in a grassland environment (Birkeland, 1984). Thus the surface deposit across the entire study site is late Holocene in age, and this is supported by radiocarbon dates from the modern C horizon of ~2250 cal yr. BP. The stacked (or buried) entisols south of the fault zone also do not represent any significant time of soil development. All of the buried soils encountered south of the fault zone are poorly developed, and appear to have not been exposed at the ground surface for an appreciable amount of time. However, these soil ages are cumulic, dependant upon the age of the overlying sediments. Given the similar soil properties observed in each of the stacked (or buried) soil profiles encountered south of the

fault zone, it is estimated that each buried entisol represents a similar time interval of around 2000 years.

Although no charcoal was found in the northern end of the trench exposure, the strongly developed buried soil profile provides a means to assess the exposure time for the soil to form, and therefore a minimum age of the underlying parent material. Based on several observations and a comparison of the soil characteristics to other published and unpublished soils ages, we interpret this soil to be late Pleistocene in age. First, the depth of clay laminae in the laminar BC horizon implies a wetting depth greater than 12 feet. Wetter middle to late Pleistocene paleoclimates provide enough precipitation to drive clay to these depths (Smiley, 1991). However, depths of average Holocene storm wetting fronts typically do not exceed ~3 to ~6 feet in southern California coastal environments. Second, the thickness of the argillic horizons in this exposure are consistent with other described and dated Pleistocene soil profiles developed under similar climatic regimes and in similar parent material (WLA, 1999; WLA, 2000; Earth Consultants International, 1999; and Lowney and Associates, 2000). Lastly, the volume and depth of translocated clay within the argillic horizons is indicative of a Pleistocene soil profile. Similar argillic horizon sequences that are on the order of 10 to 20 feet thick in West Hollywood, California are over 100,000 years old in age. At a minimum, it takes approximately 10,000 years to form a thin, juvenile (weak) argillic horizon in sandy deposits along the southern California coast (Rockwell, 1983). A significant longer period of time is required to develop the buried soil described in the north end of the trench. While we have not developed a rigorous soil chronosequence to estimate the absolute age of the soil, the strong characteristics of this soil profile imply a late Pleistocene age that is at least several tens of thousands of years to possibly one hundred thousand years or more.

The soils profiles described for this study have characteristics that vary widely across the fault zone from north to south. The two distinctly different soil types (several buried entisols versus a buried alfisol) have an abrupt contact between themselves separated by the fault zone (Figure 9). The trench and arroyo exposures were not long enough to discern if any tilting or warping affected these soil profiles. The nature of the soil profiles that have developed across the fault zone in this area does indicate that a significant amount of vertical movement occurs on this fault. Surfaces on the north side of the fault are older and therefore more stable than surfaces on the south side of the fault. This suggests that the north side of the fault has been recurrently uplifted out of the reach of ancestral Arroyo Simi and the south side of the fault has been recurrently down dropped effectively allowing little time for soil development between erosional and/or depositional events

Soil Profile Description
Arroyo Simi Exposure
Station - 2

Classification: Dystric to Typic Xerothents (stacked)
Location: Simi Valley, Ventura County, CA. Exposure station -2.
Geomorphic Surface: River terrace along West flank of Arroyo Simi
Parent Material: Late Eocene to Oligocene Sespe Formation, and terrace deposits
Vegetation: Grass land and coastal sage scrub
Described By: John Helms on 4/6/00
Exposure Type: Fresh, erosional slump failure in Arroyo wall.

Horizon	Depth (cm)	Thickness (cm)	Description
A_p	0 - 20	20	Dark grayish brown (2.5Y to 10YR 4/2 d; 2.5Y to 10YR 3/2 m); sandy loam; single grained to weak, very fine to fine, granular to subangular blocky; slightly hard, friable, non- to slightly sticky, non-plastic; 10-25%, fine to medium, rounded to sub-rounded gravel; common to many very fine to medium pores; common to many rootlets and common roots; plowed zone or locally derived fill; abrupt smooth boundary to:
A	20 - 75	55	Dark grayish brown (2.5Y to 10YR 4/2 d, 2.5Y to 10YR 3/2 m); loam to sandy loam; weak to moderate, medium, angular blocky; soft to slightly hard, friable, non-sticky, non-plastic; 0-10%, fine, sub-rounded gravel; few to common very fine to fine pores; few rootlets; gradual wavy boundary to:
C	75 - 155	80	Light olive brown (2.5 Y 5/3 d, 2.5Y 4/3 m); loamy sand, massive to single grained, very fine, granular; soft, loose, very friable, non-sticky, non-plastic; 0-5%, very fine to fine, sub-rounded gravel; well oxidized medium-grained, moderately-sorted sand; carbonate stage 0 to 1-, localized zones of disseminated calcium carbonate in matrix; extremely bioturbated, nested burrows; erosional contact with underlying buried soil; abrupt smooth boundary to:
$2A_b$	155 - 195	40	Grayish brown (10YR 5/2 d; 10YR 4/2 m); loam; weak, fine, angular blocky; hard, friable to firm, slightly sticky, moderately plastic; ~10%, fine, sub-rounded gravel; common fine pores; carbonate stage 2, nodules and disseminated calcium carbonate in matrix; localized oxidized root casts present; gradual irregular boundary to:

Horizon	Depth (cm)	Thickness (cm)	Description
2C / 2E$_b$	195 - 210	15	Light olive brown (2.5Y 5/3 d, 2.5Y 4/2 m); sandy loam; weak, fine, angular blocky; hard, friable, non-sticky, non-plastic; 0-5%, fine, sub-rounded gravel; carbonate stage 1- to 1, disseminated calcium carbonate in matrix; well-oxidized, medium-grained, moderately-sorted sand; clear wavy boundary to:
3A$_{b2}$	210 - 262	52	Brown (10YR 4/3 d; 10YR 3/3 m); loam to clay loam; moderate, medium, angular blocky; slightly hard to hard, firm, moderately sticky, moderately plastic; 10-25%, fine to medium, rounded gravel; silt or humus films (very dark grayish brown [10YR 3/2 d, 10YR 2/2 m]) few thin lining pores, few to common thin to moderately thick coating ped faces; carbonate stage 1 to 1+, localized nodules and disseminated calcium carbonate in matrix; few fine pores; fine-grained, well-sorted, well-oxidized sand; gradual irregular boundary to:
3AC$_{ox}$	262 - ?	?	Yellowish brown (10YR 5/4 d, 10YR 4/4); sandy loam; massive to weak, fine to medium, angular blocky; hard, friable, non-sticky, non-plastic; carbonate stage 1- to 1, disseminated calcium carbonate in matrix; 0-5%, fine, sub-rounded gravel; fine-grained, well-sorted, well-oxidized sand.

Soil Profile Description
Arroyo Simi Exposure
Station - 7

Classification: Dystric to Typic Xerothents (stacked)
Location: Simi Valley, Ventura County, CA. Exposure station -7.
Geomorphic Surface: River terrace along West flank of Arroyo Simi
Parent Material: Late Eocene to Oligocene Sespe Formation, and terrace deposits
Vegetation: Grass land and coastal sage scrub
Described By: John Helms on 4/6/00
Exposure Type: Fresh, erosional slump failure in Arroyo wall.

Horizon	Depth (cm)	Thickness (cm)	Description
A$_p$	0 - 18	18	Dark grayish brown (2.5Y to 10YR 4/2 d; 2.5Y to 10YR 3/2 m); sandy loam; single grained to weak, very fine to fine, granular; slightly hard, friable, non- to slightly sticky, non-plastic; 10-25%, fine to medium, rounded to sub-rounded gravel; common to many very fine to medium pores; common to many rootlets and common roots; plowed zone or locally derived fill; abrupt smooth boundary to:
A	18 - 70	52	Dark grayish brown (2.5Y to 10YR 4/2 d, 2.5Y to 10YR 3/2 m); loam to sandy loam; weak to moderate, medium, angular blocky; soft to slightly hard, friable, non-sticky, non-plastic; 0-10%, fine, sub-rounded gravel; few to common very fine to fine pores; few rootlets; gradual wavy boundary to:
C	70 - 205	125	Light olive brown (2.5 Y 5/3 d, 2.5Y 4/3 m); loamy sand, massive to single grained, very fine, granular; soft, loose, very friable, non-sticky, non-plastic; 0-5%, very fine to fine, sub-rounded gravel; well-oxidized medium-grained, moderately-sorted sand; carbonate stage 0 to 1-, localized zones of disseminated calcium carbonate in matrix; erosional contact with underlying buried soil; abrupt smooth boundary to:
2A$_b$	205 - 228	23	Dark grayish brown (10YR 4/2 d; 10YR 3/2 m); loam; weak to moderate, fine to medium, angular blocky; slightly hard to hard, friable to firm, moderately sticky, slightly plastic; 0-5%, fine, sub-rounded gravel; thin silt or humus films (very dark grayish brown [10YR 3/2 d, 10YR 2/2 m]) very few lining pores, few thin films coating ped faces; many fine pores; carbonate stage 1- to 1, localized zones of disseminated calcium carbonate in matrix; gradual irregular boundary to:

Horizon	Depth (cm)	Thickness (cm)	Description
2C / 2E$_b$	228 - 243	15	Light grayish brown (10YR 6/2 d, 10YR 5/1 m); loamy sand to sandy loam; massive to weak, fine to medium, angular blocky; loose, very friable to friable, slightly sticky, non-plastic; 0-5%, fine, sub-rounded gravel; well-oxidized medium-grained, moderately-sorted sand; clear smooth boundary to:
3A$_{b2}$	243 - 308	65	Grayish brown (10YR 5/2 d; 10YR 4/1 m); loam; massive to weak, very fine to fine, angular blocky; soft to slightly hard, friable, slightly sticky, non-plastic; 0-5%, fine, sub-rounded gravel; very few thin silt or humus films lining pores, coating ped faces, and staining grains (very dark grayish brown [10YR 3/2 d, 10YR 2/2 m]); common to many fine pores; fine-grained, well-sorted, well-oxidized sand; gradual irregular boundary to:
3AC$_{ox}$	308 - ?	?	Brown (10YR 4/3 d, 10YR 3/3); loam; massive to weak, fine to medium, angular blocky; slightly hard, friable to firm, slightly sticky, moderately plastic; 0-5%, fine, sub-rounded gravel; few to common fine pores; fine-grained, well-sorted, very well-oxidized sand.

Soil Profile Description
Trench Exposure
North Wall

Classification: Dystric to Typic Xerothent over a truncated Typic Palexeralf
Location: Simi Valley, Ventura County, CA. North Wall of Trench.
Geomorphic Surface: River terrace along West flank of Arroyo Simi
Parent Material: Late Eocene to Oligocene Sespe Formation, and terrace deposits
Vegetation: Grass land and coastal sage scrub
Described By: John Helms on 6/29/00
Exposure Type: Trench Excavation, northern wall at northern end of trench (not logged).

Horizon	Depth (cm)	Thickness (cm)	Description
A_p	0 - 20	20	Dark grayish brown (10YR 4/2 d; 10YR 2/2 m); sandy loam; moderately strong, coarse to very coarse, sub-angular blocky; very hard, friable, slightly sticky, non- to slightly plastic; 0-3%, fine to coarse, rounded to sub-rounded gravel; very fine-grained, well-sorted sand; few fine to medium pores; common rootlets and roots; organics (humus) complexed in soil matrix; many krotovena; gradual wavy boundary to:
A_1	20 - 60	40	Dark grayish brown to brown (2.5Y 4/2-3 d, 10YR 3/2 m); sandy loam; weak, medium to coarse, sub-angular blocky; hard, friable, slightly sticky, non- to slightly plastic; no gravel; fine-grained, moderately-sorted sand; few fine pores; few rootlets; organics (humus) complexed in soil matrix; many krotovena; clear wavy boundary to:
A_2	60 - 85	25	Dark grayish brown (10YR 4/2 d, 10YR 3/2-3 m); sandy loam to loam; weak, fine to medium, angular blocky; slightly hard, friable, slightly sticky, slightly plastic; no gravel; fine-grained, well-sorted sand; slight organics (humus) complexed in soil matrix; gradual wavy boundary to:
C_1	85 – 105	20	Light yellowish brown (2.5 Y 6/4 d, 2.5Y 4/4 m); loamy sand; weak, fine to medium, angular blocky; slightly hard, very friable, non-sticky, non-plastic; no gravel; fine-grained, well-sorted sand; carbonate stage 1-, disseminated calcium carbonate in soil matrix; few fine pores; clear smooth boundary to:

Horizon	Depth (cm)	Thickness (cm)	Description
2B$_{tb1}$	105 - 160	55	Yellowish brown (10YR 5/4 d, 10YR 3/4 m); loam; massive to weak, fine to medium, angular blocky; hard to very hard, friable to firm, slightly sticky, slightly plastic; no gravel; very fine-grained, well-sorted sand; carbonate stage 1-, calcium carbonate veinlets on ped faces and few nodules in soil matrix; clay films [yellowish brown (10YR 4/4 d, 10YR 3/4 m)] common thin on ped faces and lining pores, very few moderately thick on ped faces; few roots and rootlets; many fine pores; gradual wavy boundary to:
2B$_{tkb}$	160 - 270	110	Dark yellowish brown (10YR 4/4 d; 10YR 3-4/6 m); sandy clay; massive to weak, fine to medium, prismatic to angular blocky; very hard, very firm, moderately sticky, moderately plastic; ~3% fine rounded to sub-rounded gravel; very fine-grained, moderately- to well-sorted sand; carbonate stage 1, calcium carbonate veins and nodules along fractures and on ped faces; clay films [brown (7.5YR 4/4 d, 10YR 3/3 m)] many thin and common thick on ped faces, common moderately thick lining pores, and common thin bridging sand grains; gradual wavy boundary to:
2B$_{tb2}$	270 - 310	40	Brown (7.5YR 4/4-6 d, 10YR 4/3 m); clay loam; massive to weak, fine to medium, angular blocky; hard, firm to very firm, moderately sticky, moderately plastic; no gravel; very fine-grained, well-sorted sand; clay films [brown (7.5YR 4/3 d, 7.5YR 3/3 m)] many thin and common thick on ped faces, common moderately thick lining pores, and common thin bridging sand grains; clear wavy boundary to:
2BC$_{b lam1}$	310 - 374	64	Dark yellowish brown (10YR 4/6 d, 10YR 4/4 m); sandy loam to sandy clay loam; massive to weak, medium to coarse, angular blocky; slightly hard, very friable, slightly sticky, non-plastic; no gravel; fine-grained, moderately-sorted, well-oxidized sand; clay laminae [yellowish brown (10YR 5/4 d, 10YR 4/3 m)]; 1 to 7 cm thick, spaced 5 to 20 cm apart; gradual wavy boundary to:
2BC$_{b lam2}$	374 - 414	40	Dark yellowish brown (10YR 4/6 d, 10YR 4/4 m); sandy loam; massive to weak, coarse, angular blocky; soft to slightly hard, very friable, non-sticky, non-plastic; no gravel; fine-grained, moderately-sorted, well-oxidized sand; clay laminae [yellowish brown (10YR 5/4 d, 10YR 4/3 m)]; 1 to 3 cm thick, spaced 10 to 30 cm apart; clear wavy boundary to:

Horizon	Depth (cm)	Thickness (cm)	Description
2C$_{b\ ox}$	414 - ?	?	Dark yellowish brown (10YR 4/6 d, 10YR 5/4 m); loamy sand; massive, single grained; soft, very friable, non-sticky, non-plastic; no gravel; fine-grained, moderately-sorted, well-oxidized sand; undetermined lower boundary.

Soil Profile Description
Trench Exposure
Station 6, East Wall

Classification: Dystric to Typic Xerothents (stacked)
Location: Simi Valley, Ventura County, CA. East Wall of Trench.
Geomorphic Surface: River terrace along West flank of Arroyo Simi
Parent Material: Late Eocene to Oligocene Sespe Formation, and terrace deposits
Vegetation: Grass land and coastal sage scrub
Described By: John Helms on 6/29/00
Exposure Type: Trench Excavation, eastern wall at station 6 (not logged).

Horizon	Depth (cm)	Thickness (cm)	Description
A_p	0 - 20	20	Very dark grayish brown (10YR 3/2 d; 10YR 3/2 m); sandy loam; moderate, medium to coarse, angular blocky; hard to very hard, friable, slightly sticky, non-plastic; 0-3%, fine and coarse, sub-rounded gravel; very fine-grained, moderately-sorted sand; few very fine to medium pores; many rootlets and few roots; plowed zone or locally derived fill; organics (humus) complexed in soil matrix; many krotovina; abrupt wavy boundary to:
A	20 - 65	45	Dark grayish brown (2.5Y 4/2 d, 10YR 3/1 m); loamy sand; weak, fine to medium, angular blocky; slightly hard, very friable, non-sticky, non-plastic; no gravel; fine-grained, moderately-sorted sand; many fine pores; few rootlets; organics (humus) complexed in soil matrix; many krotovena; gradual wavy boundary to:
A_2	65 - 103	38	Light yellowish brown (2.5 Y 6/3 d, 2.5Y 4/2 m); sandy loam to loam; weak, fine to medium, angular blocky; slightly hard to hard, friable, slightly sticky, non- to slightly plastic; no gravel; very fine-grained, well-sorted sand; carbonate stage 1-, few veinlets of calcium carbonate on ped faces; few fine pores; few rootlets; slight organics (humus) complexed in soil matrix; common to many krotovina; diffuse wavy boundary to:
$C_{1?}$	103 - 118	15	Light yellowish brown (2.5 Y 6/3 d, 2.5Y 5/3 m); loam; massive to weak, fine to medium, angular blocky; slightly hard, friable to firm, slightly sticky, non-plastic; no gravel; very fine-grained, well sorted sand; carbonate stage 1-, few veinlets of calcium carbonate in soil matrix; few fine pores; common krodovena; clear wavy boundary to:

Horizon	Depth (cm)	Thickness (cm)	Description
2C$_{2?}$ / 2A$_{b1?}$	118 - 133	15	Light olive brown (2.5Y 5/3 d, 2.5Y 3/3 m); loam; massive to weak, fine to medium, angular blocky; slightly hard, firm, slightly sticky, slightly plastic; no gravel; very fine-grained, well sorted sand; mottled matrix [strong brown (7.5YR 5/6, 7.5YR 3/4)]; abrupt smooth boundary to:
2A$_{b1/b2}$	133 - 204	71	Grayish brown (10YR 5/2 d; 10YR 3/2 m); loam; massive to weak, fine to medium, angular blocky; slightly hard, firm, moderately sticky, moderately plastic; no gravel; very fine-grained, well-sorted sand; mottled matrix [strong brown (7.5YR 4/6, 7.5YR 3/4)] near top of horizon; carbonate stage 1--, slight calcium carbonate disseminated on ped faces; common fine pores; many rootlets along ped faces; gradual wavy boundary to:
2AB$_{kb}$	204 - 244	40	Grayish brown (10YR 5/2 d, 10YR 4/2 m); sandy loam to loam; weak, fine to medium, angular blocky; slightly hard, friable, slightly sticky, non-plastic; no gravel; very fine-grained, well-sorted sand; few faint mottles [strong brown (7.5YR 4/6 d, 7.5YR 3/4 m)]; carbonate stage 1, common calcium carbonate veinlets and nodules along ped faces; few fine pores; gradual wavy boundary to:
3Ab	244 - 256	12	Light olive brown (2.5 Y 5/3 d, 2.5Y 4/2 m); loam; weak, fine to medium, sub-angular blocky; soft to slightly hard, firm, slightly sticky, moderately plastic; no gravel; very fine-grained, very well-sorted sand; few faint mottles [dark yellowish brown (10YR 4/6 d, 10YR 3/6 m)]; carbonate stage 1--, very few calcium carbonate nodules on ped faces; few rootlets; few fine pores; gradual wavy boundary to:
3C	256 - 264	8	Light olive brown (2.5 Y 5/3 d, 2.5Y 4/3 m); loam to silt loam; massive to weak, fine to medium, angular blocky; soft, firm, slightly sticky, moderately plastic; no gravel; very fine-grained, very well-sorted sand; abrupt wavy boundary to:
4Ab	264 - 274	10	Light olive brown (2.5 Y 5/3 d, 2.5Y 4/3 m); loam to silt loam; weak, fine to medium, sub-angular blocky; soft, very firm, slightly to moderately sticky, moderately plastic; no gravel; very fine-grained, very well-sorted sand; few to common mottles [yellowish brown (10YR 5/8 d, 10YR 4/6 m) and strong brown (7.5YR 4/6 d, 7.5YR 3/4)]; few rootlets; few fine pores; gradual wavy boundary to:

A-11

Horizon	Depth (cm)	Thickness (cm)	Description
4C	274 - 284	10	Light yellowish brown (2.5 Y 6/3 d, 2.5Y 5/3 m); loam; massive to weak, fine to medium, sub-angular blocky; soft, firm, slightly sticky, slightly plastic; no gravel; very fine-grained, very-well sorted sand; very few faint mottles [yellowish brown (10YR 5/8 d, 10YR 4/6 m) and strong brown (7.5YR 4/6 d, 7.5YR 3/4)]; few rootlets; abrupt wavy boundary to:
5Ab	284 - 334	50	Light yellowish brown (2.5 Y – 10 YR 4/4 d, 10YR 4/2 m); loam to clay loam; massive to weak, fine to medium, sub-angular to angular blocky; soft, firm, moderately sticky, moderately plastic; no gravel; very fine-grained, very well sorted sand; very few faint mottles near top of horizon [yellowish brown (10YR 5/8 d, 10YR 4/6 m)]; clay films, very few thin lining pores, very few to few on ped faces; few rootlets near top of horizon; very few very fine pores; gradual wavy boundary to:
5C1	334 - 408	74	Pale yellow (2.5 Y 7/3 d, 2.5 Y 5/4 m); sand; massive to single grained, granular; soft to loose, very friable, non-sticky, non-plastic; ~3% fine, rounded gravel; fine- to medium-grained, moderately-sorted, slightly-oxidized sand; no bedding; abrupt wavy boundary to:
5C2	408 - 415	7	Brown (n.d. d, 7.5YR 5/4 m); clay; massive; soft, very firm, moderately sticky, very plastic; no gravel; very fine-grained, very well-sorted sand; primary clay with faint bedding; abrupt wavy boundary to:
5C3	415 - ?	?	Very dark grayish brown (n.d. d, 10YR 3/2 m); clay; massive; soft, very to extremely firm, moderately sticky, very plastic; no gravel; very fine-grained, very well sorted-sand; primary clay with no bedding; undetermined lower boundary.